

ACTIVATION ENERGIES OF GLOBAL REACTIONS
IN LAMINAR FLAME PROPAGATION

Thesis by
Darrell L. Ritter
Major, United States Marine Corps

In Partial Fulfillment of the Requirements
For the Degree of
Aeronautical Engineer

California Institute of Technology
Pasadena, California

1953

ACKNOWLEDGEMENTS

The author is indebted to Dr. S. S. Penner for suggesting the topic and for helpful suggestions and aid during the course of the work.

The author is also indebted to Mr. Norman Schroeder for the drafting of the figures.

ABSTRACT

A survey of experimentally determined values for the laminar burning velocity of premixed, laminar hydrocarbon-air and hydrogen-oxygen-nitrogen flames shows considerable scatter between results obtained by different investigators. Within the limits of experimental reproducibility of burning velocities, it is possible to correlate measured burning velocities on the assumption that a single rate-controlling or global reaction exists. Correlation of experimental data by use of a global reaction has been made on the basis of two simplified relations for the laminar burning velocity.

The first relation was obtained by the use of an intuitive argument based on the idea that the laminar burning velocity is proportional to the square root of a second order reaction rate, with the rate-controlling reaction step depending on the first power of the initial fuel and oxygen concentrations. For lean mixtures the global activation energy was found to have a value of about 22 Kcals/mole, and for rich mixtures it has a value of roughly 56 Kcals/mole.

The second expression for the calculation of laminar burning velocity is based on a theoretical equation derived by Semenov for a thermal mechanism controlling flame propagation in rich hydrocarbon-air mixtures. Application of this relation leads to the conclusion that a global reaction with an activation energy of 87 Kcals/mole correlates rich hydrocarbon-air burning velocities, well within the limits of reproducibility of experimental data.

A study of the effect of the concentration of N_2 in the oxidizing mixture shows an apparent dependence of the global activation energy on the amount of diluent gas. This observation suggests that although good correlation of experimental data has been obtained, by using the concept of a global activation energy, the results are not of fundamental significance but should be regarded simply as useful empirical methods for correlating experimental data. It is possible that additional theoretical work will lead to a modified expression for the laminar burning velocity, which not only permits correlation of experimental data, but also yields a global activation energy which is independent of the concentration of inert diluents.

TABLE OF CONTENTS

PART	TITLE	PAGE
	Acknowledgements	
	Abstract	
	Table of Contents	i
	List of Figures	ii - iv
	Symbols	v
I.	INTRODUCTION	1
II.	LINEAR BURNING VELOCITY AND ACTIVATION ENERGY FOR THE GLOBAL REACTION ASSUMING A SECOND-ORDER RATE-CONTROLLING REACTION STEP PROPORTIONAL TO THE FIRST POWER OF THE INITIAL FUEL AND OXYGEN CONCENTRATIONS	3
IIA.	GLOBAL REACTIONS IN HYDROCARBON-AIR MIXTURES	5
IIB.	THE GLOBAL REACTION IN RICH OR STOICHIOMETRIC HYDROGEN-OXYGEN-NITROGEN MIXTURES	7
III.	ACTIVATION ENERGIES FOR THE GLOBAL REACTION IN RICH HYDROCARBON-AIR FLAMES OBTAINED FROM THE SEMENOV EQUATION	8
IIIA.	THE GLOBAL REACTIONS IN RICH HYDROCARBON-AIR MIXTURES, USING THE SEMENOV EQUATION	10
IV.	GLOBAL REACTIONS IN HYDROCARBON-OXYGEN-NITROGEN FLAMES ($\alpha \neq 0.21$)	10
IVA.	GLOBAL ACTIVATION ENERGY FOR $\alpha \neq 0.21$, CALCULATED FROM EQUATION (6b)	11
IVB.	GLOBAL ACTIVATION ENERGY FOR $\alpha \neq 0.21$, CALCULATED FROM THE SEMENOV EQUATION (11)	12
	References	13 - 15
	Table I	16
	Table II	17

LIST OF FIGURES

FIGURE	TITLE	PAGE
1	Burning Velocities of Methane-Air Mixtures as a function of Mixture Ratio	18
2	Burning Velocities of Propane-Air Mixtures as a Function of Mixture Ratio	19
3	Burning Velocities of Ethylene-Air Mixtures as a Function of Mixture Ratio	20
4	Burning Velocities of Acetylene-Air Mixtures as a Function of Mixture Ratio	21
5	Plot of $\ln \left[100 \text{ Su} (1 + \alpha r \phi) / \phi^{1/2} T_c \right]$ vs. $10^4 / T_c$ for Methane-Air Flames	22
6	Plot of $\ln \left[100 \text{ Su} (1 + \alpha r \phi) / \phi^{1/2} T_c \right]$ vs. $10^4 / T_c$ for Ethane-Air Flames	23
7	Plot of $\ln \left[100 \text{ Su} (1 + \alpha r \phi) / \phi^{1/2} T_c \right]$ vs. $10^4 / T_c$ for Propane-Air Flames	24
8	Plot of $\ln \left[100 \text{ Su} (1 + \alpha r \phi) / \phi^{1/2} T_c \right]$ vs. $10^4 / T_c$ for Pentane-Air Flames	25
9	Plot of $\ln \left[100 \text{ Su} (1 + \alpha r \phi) / \phi^{1/2} T_c \right]$ vs. $10^4 / T_c$ for Ethylene-Air Flames	26
10	Plot of $\ln \left[100 \text{ Su} (1 + \alpha r \phi) / \phi^{1/2} T_c \right]$ vs. $10^4 / T_c$ for Acetylene-Air Flames	27
11	Plot of $\ln \left[100 \text{ Su} (1 + \alpha r \phi) / \phi^{1/2} T_c \right]$ vs. $10^4 / T_c$ for Propyne-Air Flames	28
12	Plot of $\ln \left[100 \text{ Su} (1 + \alpha r \phi) / \phi^{1/2} T_c \right]$ vs. $10^4 / T_c$ for 2, 2, 4-Trimethylpentane Flames	29
13	Plot of $\ln \left[100 \text{ Su} (1 + \alpha r \phi) / \phi^{1/2} T_c \right]$ vs. $10^4 / T_c$ for Benzene-Air Flames	30
14	Summary Plot for the Determination of the Activation Energy of the Global Reaction for Lean Hydrocarbon-Air Mixtures	31

LIST OF FIGURES (Cont'd)

FIGURE	TITLE	PAGE
15	Summary Plot for the Determination of the Activation Energy of the Global Reaction for Rich Hydrocarbon-Air Mixtures	32
16	Plot of $\ln \left[100 \text{ Su} (1 + \alpha r \phi) / \phi^{1/2} \alpha T_c \right]$ vs. $10^4 / T_c$ for $\text{H}_2 - \text{O}_2 - \text{N}_2$ Flames	33
17	Plot of $\ln \left[100 \text{ Su} (T_c - T_o) (1 + \alpha r \phi)^{1/2} / T_c (1 + 0.9 / \phi)^{1/2} \right]$ vs. $10^4 / T_c$ for Methane-Air Flames	34
18	Plot of $\ln \left[100 \text{ Su} (T_c - T_o) (1 + \alpha r \phi)^{1/2} / T_c (1 + 0.9 / \phi)^{1/2} \right]$ vs. $10^4 / T_c$ for Ethane-Air Flames	35
19	Plot of $\ln \left[100 \text{ Su} (T_c - T_o) (1 + \alpha r \phi)^{1/2} / T_c (1 + 0.9 / \phi)^{1/2} \right]$ vs. $10^4 / T_c$ for Propane-Air Flames	36
20	Plot of $\ln \left[100 \text{ Su} (T_c - T_o) (1 + \alpha r \phi)^{1/2} / T_c (1 + 0.9 / \phi)^{1/2} \right]$ vs. $10^4 / T_c$ for Pentane-Air Flames	37
21	Plot of $\ln \left[100 \text{ Su} (T_c - T_o) (1 + \alpha r \phi)^{1/2} / T_c (1 + 0.9 / \phi)^{1/2} \right]$ vs. $10^4 / T_c$ for Ethylene-Air Flames	38
22	Plot of $\ln \left[100 \text{ Su} (T_c - T_o) (1 + \alpha r \phi)^{1/2} / T_c (1 + 0.9 / \phi)^{1/2} \right]$ vs. $10^4 / T_c$ for Acetylene-Air Flames	39
23	Plot of $\ln \left[100 \text{ Su} (T_c - T_o) (1 + \alpha r \phi)^{1/2} / T_c (1 + 0.9 / \phi)^{1/2} \right]$ vs. $10^4 / T_c$ for Benzene-Air Flames	40
24	Summary Plot of Rich Hydrocarbon-Air Flames	41
25	Plot of Su vs. α for Propane-Oxygen-Nitrogen Mixtures ($T_i = 311^\circ\text{K}$)	42
26	Plot of Su vs. α for Propane-Oxygen-Nitrogen Mixtures ($T_i = 422^\circ\text{K}$)	43
27	Plot of Su vs. α for Ethylene-Oxygen-Nitrogen Mixtures ($T_i = 311^\circ\text{K}$)	44

LIST OF FIGURES (Cont'd)

FIGURE	TITLE	PAGE
28	Plot of S_u vs. α for Ethylene-Oxygen-Nitrogen Mixtures ($T_i = 422^\circ\text{K}$)	45
29	Plot of $\ln \left[100 S_{u_{\max}} (1 + \alpha r \phi) / \phi^{1/2} T_c \alpha \right]$ vs. $10^4/T_c$ for Propane- O_2 - N_2 Flames	46
30	Plot of $\ln \left[100 S_{u_{\max}} (1 + \alpha r \phi) / \phi^{1/2} T_c \alpha \right]$ vs. $10^4/T_c$ for Ethylene- O_2 - N_2 Flames	47
31	Plot of $\ln \left[100 S_{u_{\max}} (T_c - T_o) (1 + \alpha r \phi)^{1/2} / T_c \alpha^{1/2} (1 - 0.9/\phi)^{1/2} \right]$ vs. $10^4/T_c$ for Propane- O_2 - N_2 Flames	48
32	Plot of $\ln \left[100 S_{u_{\max}} (T_c - T_o) (1 + \alpha r \phi)^{1/2} / T_c \alpha^{1/2} (1 - 0.9/\phi)^{1/2} \right]$ vs. $10^4/T_c$ for Ethylene- O_2 - N_2 Flames	49

SYMBOLS

a	fuel concentration, molecules/cm ³
b	oxygen concentration, molecules/cm ³
\bar{c}_p	mean specific heat, T_o to T_c , cal/(g)(°K)
c_p	molar heat capacity at constant pressure, cal/(mole)(°K)
D	diffusion coefficient, cm ² /sec
E	activation energy, Kcal/mole
N_F	total number of moles of fuel
N_{N_2}	total number of moles of nitrogen
N_{O_2}	total number of moles of oxygen
n_r/n_p	moles of reactants per moles of products from stoichiometric equation
P	steric factor
p	total pressure
R	molar gas constant
r	stoichiometric molar fuel to oxygen ratio
T	absolute temperature, °K
S_u	flame velocity, cm/sec
Z	collision number
α	mole fraction of oxygen in oxygen-nitrogen mixture
λ	thermal conductivity
ρ	density of mixture
ϕ	equivalence ratio, fraction of stoichiometric fuel-oxygen ratio

Subscripts:

o, i	initial condition
c	condition at flame temperature
eff	effective mean reactant concentration

I. INTRODUCTION

During the last few years a large number of articles describing experimental measurements of laminar burning velocity have been published. Theoretical studies have appeared which range in complexity and scope from obviously oversimplified physical pictures to very detailed theoretical studies carried out by J. O. Hirschfelder and his collaborators. ^{(i), (ii)} Although the essential features of the analytical problem are now well understood, and are described with great clarity in a paper by von Kármán and Millán, ⁽ⁱⁱⁱ⁾ the relation of simplified theories to the published experimental data has not been examined in great detail. Thus Hirschfelder and his collaborators have shown that theoretical calculations lead to excellent agreement with experimentally determined laminar burning velocities provided the detailed reaction kinetics is understood, as in the ozone flame, ⁽ⁱⁱ⁾ which was first studied by Lewis and von Elbe. ^(iv) For hydrazine and nitric oxide decomposition flames, results are obtained by making intelligent guesses about the nature of the rate-controlling reaction step. ⁽ⁱⁱ⁾ However, for the most important class of premixed laminar flames, i. e., hydrocarbon-air flames, the detailed theories of flame propagation cannot be used because the chemistry of the reaction processes is not understood quantitatively. In fact, it appears unlikely that a molecular theory of flame propagation for hydrocarbon-air flames can be developed in the foreseeable future.

In the absence of detailed kinetics data it is only reasonable to follow the suggestion of von Kármán to attempt an empirical correlation

of burning velocity data for hydrocarbon-air flames on the assumption that a global reaction exists. It is the purpose of this paper to demonstrate that the concept of a global reaction in hydrocarbon-air flames leads to useful correlations provided lean and rich mixtures are treated separately.

II. LINEAR BURNING VELOCITY AND ACTIVATION ENERGY FOR THE GLOBAL REACTION ASSUMING A SECOND-ORDER RATE-CONTROLLING REACTION STEP PROPORTIONAL TO THE FIRST POWER OF THE INITIAL FUEL AND OXYGEN CONCENTRATIONS

Theories of laminar flame propagation^(i-v) generally lead to the result that the linear burning velocity, S_u , is proportional to the square root of the specific reaction rate constant for the rate-controlling reaction step, evaluated at the adiabatic flame temperature T_c . We shall designate the quantity E appearing in the term $\exp(-E/2RT_c)$ as the activation energy for the global reaction. Experimental studies of the effect of pressure, p , on laminar burning velocity have shown either a weak dependence^(vi) for S_u on p or else suggest, particularly for hydrocarbon-air flames, that S_u is independent of pressure.^(vii) The latter results are well-known to be consistent with the idea that the rate-controlling reaction step is of the second order. For the sake of simplicity, and in the absence of quantitative information to the contrary, we shall assume that the rate-controlling reaction step is a second order reaction between fuel, F , and oxygen, O_2 , with the reaction rate determined by the initial concentrations of reactants.

Quantitative relations for S_u show that it is a function of coefficients such as an effective thermal conductivity, an effective diffusion coefficient, an average heat capacity, etc. However, it is to be expected that these quantities may be treated, in first approximation, as constants independent of T_c , for a given fuel-oxidizer system, as the mixture ratio is changed. Hence we postulate the following functional form for the laminar burning velocity

$$Su = c' T_c \left\{ (N_F) / \left[(N_{O_2}) + (N_{N_2}) + (N_F) \right] \right\}^{1/2} \left\{ (N_{O_2}) / \left[(N_{O_2}) + (N_{N_2}) + (N_F) \right] \right\}^{1/2} \times \exp(-E/2RT_c) \quad (1)$$

where the parameter c' is independent of T_c , and (N_F) , (N_{O_2}) , and (N_{N_2}) denote, respectively, the total number of moles of fuel, oxygen, and nitrogen initially present in the combustible gases. In general we expect c' to be different for different reactive gases.

Let

$$r = \left[(N_F) / (N_{O_2}) \right]_{\text{stoichiometric}} \quad (2)$$

represent the stoichiometric molar fuel to oxygen ratio. The equivalence ratio, ϕ , is then defined by the relation

$$\phi = \left[(N_F) / (N_{O_2}) \right] / r, \quad (3)$$

i. e., ϕ represents the actual molar fuel to oxygen ratio divided by the corresponding stoichiometric ratio. We also introduce a parameter α through the expression

$$\alpha = (N_{O_2}) / \left[(N_{O_2}) + (N_{N_2}) \right]. \quad (4)$$

From Eq. (3) it follows that

$$(N_F) = r (N_{O_2}) \phi$$

whence

$$(N_F)^{1/2} (N_{O_2})^{1/2} = (N_{O_2}) r^{1/2} \phi^{1/2}$$

and Eq. (1) becomes

$$Su = c \phi^{1/2} T_c \left\{ (N_{O_2}) / \left[(N_{O_2}) + (N_{N_2}) + (N_F) \right] \right\} \exp (-E/2RT_c) \quad (5)$$

where $c = c'r^{1/2}$. Replacing (N_F) by $r(N_{O_2}) \phi$ and (N_{N_2}) by $\left[(1 - \alpha)/\alpha \right] (N_{O_2})$, Eq. (5) becomes

$$Su = c \phi^{1/2} T_c \left[\alpha / (1 + \alpha r \phi) \right] \exp (-E/2RT_c). \quad (6)$$

For fixed values of α (i.e., for air) it is apparent from Eq. (6) that the activation energy for the global reaction is determined by the relation

$$E = - 2R \partial \ln \left[Su (1 + \alpha r \phi) / \phi^{1/2} T_c \right] / \partial (1/T_c) \quad (6a)$$

where α has the numerical value 0.21 for air. If α is not held constant then Eq. (6a) should be replaced by the expression

$$E = - 2R \partial \ln \left[Su (1 + \alpha r \phi) / \alpha \phi^{1/2} T_c \right] / \partial (1/T_c). \quad (6b)$$

Application of Eq. (6a) to hydrocarbon-air mixtures will be described in the following Section IIA. The use of Eq. (6b) for lean or stoichiometric hydrogen-oxygen-nitrogen mixtures is described in Section IIB.

IIA. GLOBAL REACTIONS IN HYDROCARBON-AIR MIXTURES

The attempt at correlating observed laminar burning velocities through a global reaction is greatly complicated by the lack of agreement between laminar burning velocities determined by different investigators and by the use of different experimental techniques. This last remark is amplified by reference to Figs. 1 to 4 in which laminar burning velocities Su , determined by different investigators,

are shown as a function of volume per cent of methane, propane, ethylene, and acetylene, respectively.* The volume per cent of fuel, v_F is related to the parameters α , r , and ϕ through the expression

$$v_F = 100 \alpha r \phi / (1 + \alpha r \phi). \quad (7)$$

The adiabatic flame temperature, T_c , was calculated as a function of ϕ for $\alpha = 0.21$ for various fuel to air mixtures by using standard procedures, which are, however, rather laborious to utilize.^(viii) The results of these calculations are plotted according to Eq. (6a) in Figs. 5 to 13 for methane, ethane, propane, pentane, ethylene, acetylene, propyne, 2,2,4-trimethyl pentane and benzene, respectively. Reference to the data given in Figs. 5 to 13 shows extensive scatter of the type which is to be expected on the basis of the discrepancies between the experimental data plotted in Figs. 1 to 4. Activation energies for the global reaction obtained for different fuels are listed in Table I. It is perhaps noteworthy that, in general, different activation energies seem to be required for rich and lean mixtures and that greatly different activation energies are obtained by different investigators are employed (see, for example, the acetylene-air data plotted in Fig. 10, which yield activation energies between 33 and 80 Kcals/mole for rich mixtures depending on the source of the data).

In view of the scatter of the experimentally determined burning velocities it is not unreasonable to attempt a universal correlation for all hydrocarbon-air mixtures. The desired plot may be constructed

* References referred to on the graphs are listed on reference sheet.

by shifting the calculated values of $\ln \left[Su (1 + ar\phi) / \phi^{1/2} T_c \right]$ by a fixed amount for each fuel-air system. The resulting data are shown in Figs. 14 and 15 for lean and for rich hydrocarbon-air mixtures, respectively. Reference to Figs. 14 and 15 shows that at least for rich mixtures, within the limits of reproducibility of burning velocities, it is possible to correlate measured burning velocities on the assumption that a global chemical reaction exists. For lean mixtures the global activation energy has a value of roughly 22 Kcals/mole, whereas for rich mixtures the global activation energy is about 56 Kcals/mole.

II.B. THE GLOBAL REACTION IN RICH OR STOICHIOMETRIC HYDROGEN-OXYGEN-NITROGEN MIXTURES

Burning velocities for hydrogen-oxygen-nitrogen mixtures, listed by Sachsse and Bartholomé,^(ix) have been used in connection with Eq. (6b) to estimate the activation energy for the global reaction. The resulting data are plotted in Fig. 16 and lead to a value of 6.5 Kcals/mole for E in rich mixtures. It is perhaps noteworthy that the experimental data for the stoichiometric mixture ratios do not fall close to the "best" curve drawn through the rich mixture data.

III. ACTIVATION ENERGIES FOR THE GLOBAL REACTION IN RICH HYDROCARBON-AIR FLAMES, OBTAINED FROM THE SEMENOV EQUATION

An approximate theoretical equation for laminar burning velocity, based on a thermal mechanism of energy transfer, has been given by Semenov.^(x) For a bimolecular reaction between fuel molecules and oxygen molecules, the equation may be written in the form.^(xi)

$$Su = \left\{ \left[2 \lambda P Z a_{\text{eff}} b_{\text{eff}} / a_o \rho_o \bar{C}_p (T_c - T_o) \right] (\lambda / C_p D \rho_f)^2 \right. \\ \left. x (n_r / n_p)^2 (RT_c^2 / E) \exp (-E / RT_c) \right\}^{1/2} \quad (8)$$

where, for stoichiometric or fuel-rich mixtures ($\phi \geq 1$), a_{eff} and b_{eff} are to be computed from the relations

$$\left. \begin{aligned} a_{\text{eff}} &= a_o T_o / T_c \left\{ 1 - 1/\phi \left[1 - RT_c^2 / E (T_c - T_o) \right] \right\} \\ b_{\text{eff}} &= b_o T_o / T_c \left[RT_c^2 / E (T_c - T_o) \right] \end{aligned} \right\} \quad (9)$$

The quantities a_{eff} , b_{eff} , and b_o are defined as the effective mean reactive fuel concentration, the effective mean reactive oxygen concentration, and the initial oxygen concentration, respectively.

In the first approximation we may write

$$Su = \text{constant} \times \left[T_c^2 a_{\text{eff}} b_{\text{eff}} \exp (-E / RT_c) / a_o (T_c - T_o) \right]^{1/2} \quad (10)$$

From the relations in Eq. (9) we get:

$$a_{\text{eff}} b_{\text{eff}} / a_o = (T_o / T_c)^2 b_o RT_c^2 / E (T_c - T_o) \\ \times \left\{ 1 - 1/\phi \left[1 - RT_c^2 / E (T_c - T_o) \right] \right\} \quad (9a)$$

Since $RT_c^2 / E (T_c - T_o)$ is approximately equal 0.1, Eq. (9a) becomes

$$a_{\text{eff}} b_{\text{eff}} / a_o \approx RT_o^2 b_o (1 - 0.9/\phi) / E (T_c - T_o) \quad (9b)$$

Substituting Eq. (9b) into Eq. (10) leads to the relation

$$Su = \text{constant} \times \left[T_c^2 T_o^2 R b_o (1 - 0.9/\phi) \exp(-E/RT_c) / E(T_c - T_o)^2 \right]^{1/2} \quad (10a)$$

Hence, for a given combustible mixture and fixed initial temperature, T_o ,

$$Su = \text{constant} \left[T_c^2 b_o (1 - 0.9/\phi) \exp(-E/RT_c) / (T_c - T_o)^2 \right]^{1/2} \quad (10b)$$

By definition

$$b_o = \left[N_{O_2} / (N_F + N_{O_2} + N_{N_2}) \right]_o (C_T)_o$$

where $(C_T)_o$ is the total concentration. For any fixed pressure and temperature, $(C_T)_o$ is a constant and hence Eq. (10b) may be written

$$Su = \text{constant} \times \left[T_c / (T_c - T_o) \right] (1 - 0.9/\phi)^{1/2} \left[N_{O_2} / (N_F + N_{O_2} + N_{N_2}) \right]^{1/2} \exp(-E/2RT_c). \quad (10c)$$

Utilizing Eqs. (3) and (4) developed in Section II, we get

$$N_{O_2} / (N_F + N_{O_2} + N_{N_2}) = \alpha / (1 + \alpha r \phi)$$

whence

$$Su = \text{constant} \times \left[T_c / (T_c - T_o) \right] (1 - 0.9/\phi)^{1/2} \left[\alpha / (1 + \alpha r \phi) \right]^{1/2} \exp(-E/2RT_c). \quad (10d)$$

For fixed values of α it is apparent from Eq. (10d) that the activation energy for the global reaction is determined by the relation

$$E = -2R \partial \ln \left[Su (1 + \alpha r \phi)^{1/2} (T_c - T_o) / T_c (1 - 0.9/\phi)^{1/2} \right] / \partial (1/T_c) \quad (11)$$

If α is not held constant, then Eq. (11) should be replaced by the expression

$$E = -2R \partial \ln \left[Su (1 + \alpha r \phi)^{1/2} (T_c - T_o) / T_c \alpha^{1/2} (1 - 0.9/\phi)^{1/2} \right] / \partial (1/T_c) \quad (11a)$$

Application of Eq. (11) to hydrocarbon-air mixtures will be discussed in the following section.

IIIA. THE GLOBAL REACTIONS IN RICH HYDROCARBON-AIR MIXTURES, USING THE SEMENOV EQUATION

Equation (11) was used for the determination of E by utilizing the same data that were employed in Section IIA. The results are plotted in Figs. 17 through 23 for methane, ethane, propane, pentane, ethylene, acetylene, and benzene, and the resulting activation energies are listed in Table II. In order to find a global activation energy which is applicable to all rich hydrocarbon-air mixtures, the same technique was used as has been described in Section II. These results are plotted in Fig. 24 and give an activation energy of 87 Kcal/mole.

The correlation with the experimental data appears to be quite good but the activation energy is more than half again as large as the 56 Kcal/mole which was obtained using the concept of a second-order rate-controlling reaction step proportional to the first power of the initial fuel and oxygen concentrations.

On the basis of the available data it appears justified to conclude that almost any expression for S_u containing the factor $\exp(-E/2RT_c)$ will permit empirical fitting of burning velocities for rich hydrocarbon-air flames.

IV. GLOBAL REACTIONS IN HYDROCARBON-OXYGEN-NITROGEN FLAMES ($\alpha \neq 0.21$)

Burning velocities for propane-and ethylene-oxygen-nitrogen mixtures, for various values of α , have been obtained by Dugger and Graab.^(xi) These investigators noted that the effect of α on burning velocity was predicted, within approximately 5 to 15 per cent, by simplified semi-empirical equations based either on a thermal or on an active particle diffusion mechanism for energy transfer in laminar flame propagation. However, neither theory was found to be in accord with an observed linear relation to S_u and α .*

It is of obvious interest to redetermine the global activation energies for hydrocarbon flames in which air has been replaced by various mixtures of oxygen and nitrogen. The desired correlation can be obtained by utilizing either Eq. (6b) or Eq. (11a). The results of these calculations are summarized in the following paragraphs IVA and IVB. They show considerably lower global activation energies than were obtained for combustible mixtures utilizing air as oxidizer. This result suggests that the relation used in Section II, as well as the Semenov equation employed in Section III, do not represent a fortunate functional form for the laminar burning velocity. However, it is possible that additional theoretical studies of laminar flame propagation controlled by second-order reaction steps will ultimately yield a relation that fits rich hydrocarbon flames with a global activation

* Dugger and Graab speak only of a linear relation between the maximum value of S_u (for a fixed α) and α . However, it is easily shown that the experimental data are in accord with the idea that S_u is a linear function of α for fixed values of ϕ . Representative data are shown in Figs. 25 to 28.

energy, which is independent of the amount of inert gas added to the combustible mixture.

IVA. GLOBAL ACTIVATION ENERGY FOR $\alpha \neq 0.21$, CALCULATED FROM EQUATION (6b)

The experimental data of Dugger and Graab have been used in conjunction with Eq. (6b) to obtain global activation energies. The results are plotted in Figs. 29 and 30, respectively, for propane and ethylene mixtures with oxygen and nitrogen.

Reference to Figs. 29 and 30 shows that E is appreciably less than 56 Kcals/mole, which was obtained from the universal correlation shown in Fig. 15. It is possible that this result has been produced, in part, by the fact that the data of Figs. 29 and 30 are restricted to maximum burning velocities for fixed compositions and hence to nearly stoichiometric mixtures. Nevertheless the discrepancies are so large as to suggest that Eq. (6) was not the most fortunate for correlating burning velocity data.

IVB. GLOBAL ACTIVATION ENERGY FOR $\alpha \neq 0.21$, CALCULATED FROM THE SEMENOV EQUATION (11)

The same data which were used in the construction of Figs. 29 and 30 have been used also, in connection with Eq. (11), to obtain Figs. 31 and 32. Comparison of the global activation energies determined from Figs. 31 and 32 with the universal correlation shown in Fig. 24, again leads to the conclusion that the apparent global activation energy is a sensitive function of α . Hence the remarks concerning Eq. (6) made in paragraph IVA also apply to the Semenov equation.

REFERENCES

- i. J. O. Hirschfelder and C. F. Curtiss, J. Chem. Phys. 17, 1076 (1949); J. Phys. Coll. Chem. 55, 774 (1951). C. F. Curtiss, J. O. Hirschfelder, and D. E. Campbell, Report CM-690, University of Wisconsin Naval Research Laboratory, Madison, February 1952.
- ii. J. O. Hirschfelder, C. F. Curtiss, and D. E. Campbell, Report CM-756, University of Wisconsin Naval Research Laboratory, Madison, November 1952.
- iii. Th. von Kármán and G. Millán, C. B. Biezeno Anniversary Volume on Applied Mechanics, pp. 59-69, Haarlem, March 1953.
- iv. B. Lewis and G. von Elbe, J. Chem. Phys. 2, 283 (1934); Chem. Rev. 21, 347 (1937).
- v. Ya. B. Zeldovich and D. A. Frank-Kamenetsky, Compt. rend. (Doklady) Ac. Sci. USSR 19, 693 (1938).
- vi. C. Tanford and R. N. Pease, J. Chem. Phys. 15, 431, 433, 861 (1947).
- vii. M. Gilbert, unpublished observations; H. G. Wolfhard, Zeits. f. Techn. Phys. 24, 206 (1943).
- viii. C. N. Satterfield, H. C. Hottel, and G. C. Williams, "Generalized Thermodynamics of High Temperature Combustion", M.I.T. Report No. 17, May 1947; R. W. Smith, Jr., H. E. Edwards, and S. R. Brinkley, Jr., Bureau of Mines Report 4938, January 1953.
- ix. H. Sachsse and E. Bartholomé, Zeits. f. Elektrochem, 53, 183 (1949).
- x. N. N. Semenov, NACA TM 1026, (1942).
- xi. G. L. Dugger and D. D. Graab, NACA RM E52J24, (1953).

REFERENCES ON EXPERIMENTAL BURNING VELOCITIES
TO BE USED WITH FIGURES 1 TO 32

1. J. W. Andersen and R. S. Fein, "Measurements of Normal Burning Velocities and Flame Temperatures of Bunsen Flames", J. Chem. Physics, vol. 17, pp. 1268-1273 (1949).
2. J. W. Andersen and R. S. Fein, "Measurements of Normal Burning Velocities of Propane-Air Flames by Shadow Photographs", J. of Chem. Physics, vol. 18, pp. 441-443 (1950).
3. E. Bartholomé, "Zur Methodik der Messung von Flammengeschwindigkeiten", Zeitschrift für Electrochemie, vol. 53, pp. 191-196 (1949).
4. H. R. Conan and J. W. Linnett, "Burning Velocity Determinations, Part V, The Use of Schlieren Photography in Determining Burning Velocities by the Burner Method", Transactions of the Faraday Society, vol. 47, pp. 981-988 (1951).
5. H. F. Coward and F. J. Hartwell, "Studies in Mechanism of Flame Movement. Part II. The Fundamental Speed of Flame in Mixtures of Methane and Air", J. of Chem. Society, pp. 2676-2684 (1932).
6. G. L. Dugger, "Effect of Initial Mixture Temperatures on Flame Speeds and Blow-off Limits of Propane-Air Flames", NACA TN 2170, August 1950.
7. G. L. Dugger, "Effect of Initial Mixture Temperatures on Flame Speed of Methane-Air, Propane-Air, and Ethylene-Air Mixtures", NACA TN 2374, May 1951.
8. G. L. Dugger and D. D. Graab, "Flame Speeds of 2,2,4-Trimethylpentane-Oxygen-Nitrogen Mixtures, NACA TN 2680 April 1952.
9. G. L. Dugger and D. D. Graab, "Flame Velocities of Propane- and Ethylene-Oxygen-Nitrogen Mixtures", NACA RM E52J24, January 1953.
10. F. H. Garner, R. Long, and G. K. Ashforth, "Burning Velocities of Propane-Air Mixtures", Fuel, vol. 30, pp. 63-66 (1951).
11. M. Gerstein, O. Levine, and E. L. Wong, "Fundamental Flame Velocities of Pure Hydrocarbons, I - Alkanes, Alkenes, Alkynes, Benzene, and Cyclohexane", NACA RM E50G24, September 1950.
12. O. Levine and M. Gerstein, "Fundamental Flame Velocities of Pure Hydrocarbons, III. Extension of Tube Method to High Flame Velocities of Acetylene-Air Mixtures", NACA RM E51J05 (December 1951).

13. J. W. Linnett and M. F. Hoare, "Burning Velocities in Ethylene-Air-Nitrogen Mixtures", Third Symposium on Combustion and Flame and Explosion Phenomena, The Williams and Wilkins Co. pp. 195-203 (1949).
14. J. W. Linnett, H. S. Pickering, and P. J. Wheatley, "Burning Velocity Determinations, Part IV - The Soap Bubble Method of Determining Burning Velocities", Transactions of the Faraday Society, vol. 47, pp. 974-980 (1951).
15. H. S. Pickering and J. W. Linnett, "Burning Velocity Determinations, Part VI - The Use of Schlieren Photography in Determining Burning Velocities by the Soap Bubble Method", Transactions of the Faraday Society, vol. 47, pp. 989-992 (1951).
16. H. Sachsse and E. Bartholomé, Zeits. f. Electrochem, vol. 53, pp. 183-191 (1949).
17. C. N. Satterfield, H. C. Hottel, and G. C. Williams, "Generalized Thermodynamics of High Temperature Combustion", M.I.T. Report 17, May 1947.
18. D. M. Simon and E. L. Wong, "Flame Velocities Over a Wide Composition Range for Pentane-Air, Ethylene-Air, and Propyne-Air Flames", NACA RM E51H09, October 1951.
19. F. A. Smith and S. F. Pickering, "Measurements of Flame Velocity by a Modified Burner Method", J. of Research of the National Bureau of Standards, vol. 17, pp. 7-43 (1936).
20. R. W. Smith, Jr., H. E. Edwards, and S. R. Brinkley, Jr., "The Thermodynamics of Combustion Gases: Temperatures of Methane-Air and Propane-Air Flames at Atmospheric Pressure", Bureau of Mines, Report of Investigations 4938, January 1953.
21. P. J. Wheatley and J. W. Linnett, "Burning Velocity Determinations, Part VIII - Some Acetylene + Oxygen + Inert Gas Mixtures", Transactions of the Faraday Society, vol. 48, 338 (1952).

Table I. Apparent Activation Energies for the Global Reaction in Various Hydrocarbon-Air Flames Assuming a Second-Order Rate-Controlling Reaction Step Proportional to the First Power of the Initial Fuel and Oxygen Concentrations.

Figure	Hydrocarbon	E for Rich Mixtures (Kcal/mole)	E for Lean Mixtures (Kcal/mole)
5	Methane	44, 108	32
6	Ethane	-	10
7	Propane	56, 74	0.6
8	Pentane	-	16
9	Ethylene	54	9
10	Acetylene	33, 50, 80	-
11	Propyne	-	18
12	2, 2, 4 Trimethyl Pentane	34	-
13	Benzene	58	-
14	Rich	56	-
15	Lean	-	22

Table II. Apparent Activation Energies for the Global Reaction
in Various Rich Hydrocarbon-Air Flames using the
Semenov Equation.

Figure	Hydrocarbon	E (Kcal/mole)
17	Methane	100
18	Ethane	75
19	Propane	91
20	Pentane	60
21	Ethylene	74, 30
22	Acetylene	53, 90, 117
23	Benzene	175
24	Summary	87

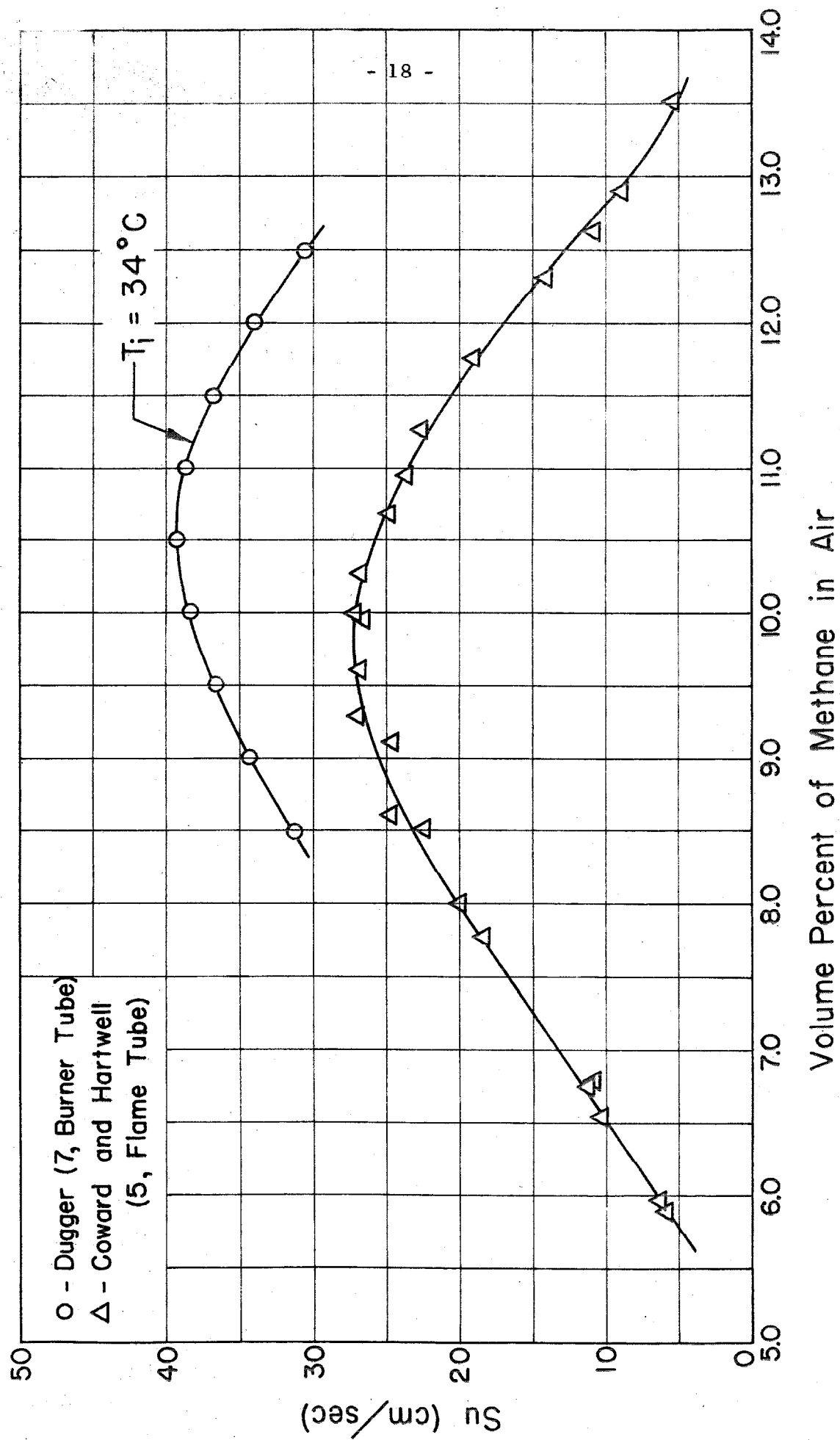


FIGURE 1. BURNING VELOCITIES OF METHANE - AIR MIXTURES AS A FUNCTION OF MIXTURE RATIO ($p=1$ ATMOS., T_i = ROOM TEMPERATURE EXCEPT AS INDICATED)

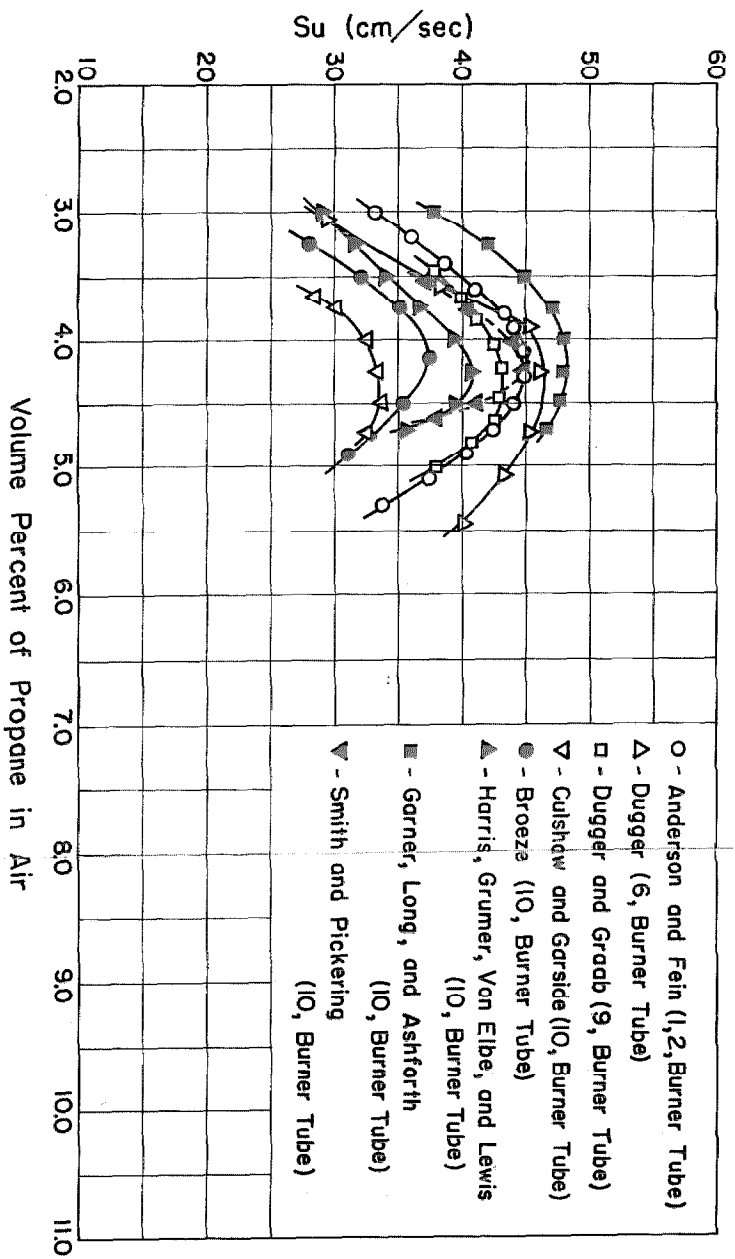


FIGURE 2. BURNING VELOCITIES OF PROPANE-AIR MIXTURES AS A FUNCTION OF MIXTURE RATIO ($p = 1$ ATMOS., $T =$ ROOM TEMPERATURE; REPLOTED FROM THE DATA GIVEN BY GARNER, LONG, AND ASHFORTH, REF. 10)

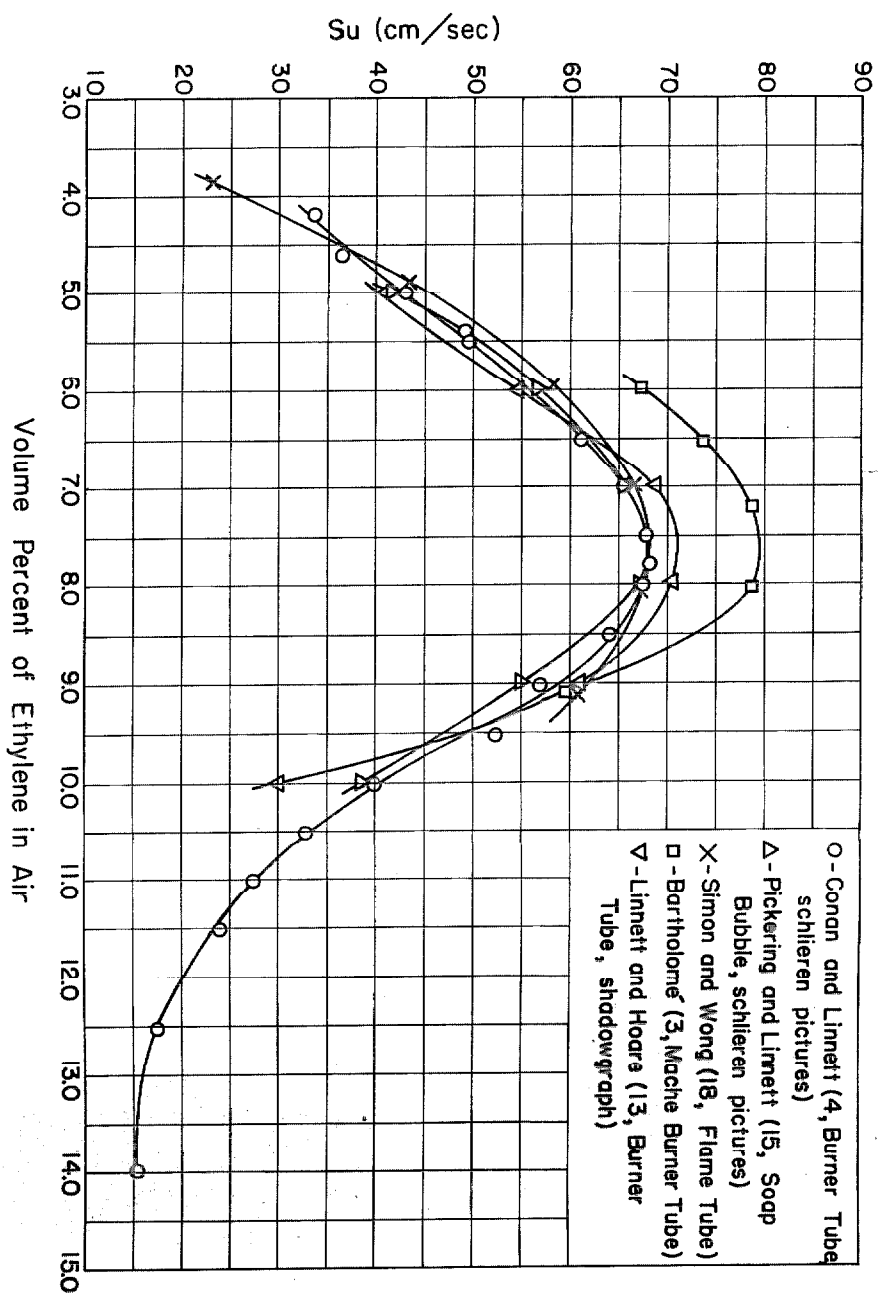


FIGURE 3. BURNING VELOCITIES OF ETHYLENE-AIR MIXTURES AS A FUNCTION OF MIXTURE RATIO ($p = 1$ ATMOS., $T_i =$ ROOM TEMPERATURE)

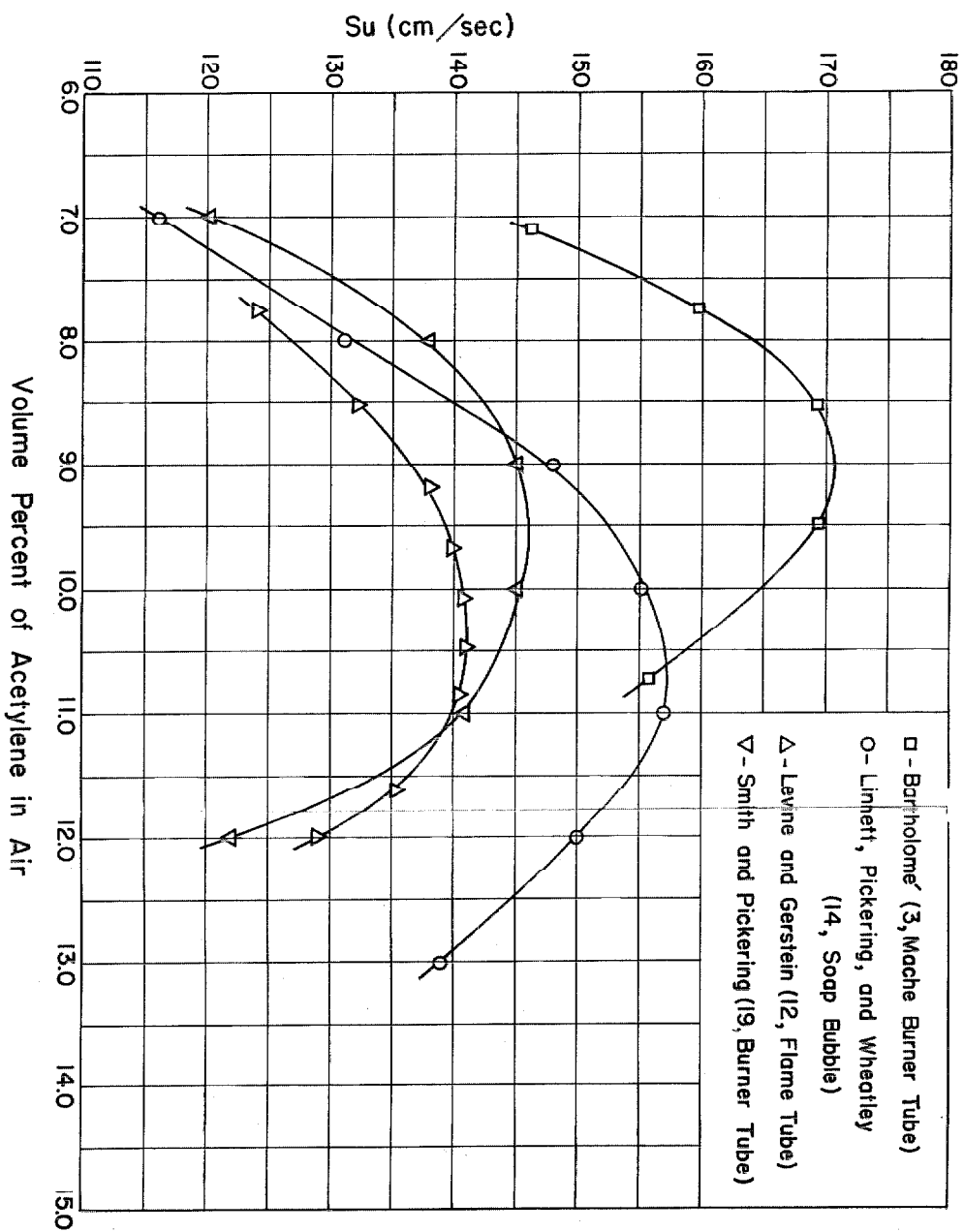


FIGURE 4. BURNING VELOCITIES OF ACETYLENE-AIR MIXTURES AS A FUNCTION OF MIXTURE RATIO ($p = 1$ ATMOS., $T_f =$ ROOM TEMPERATURE)

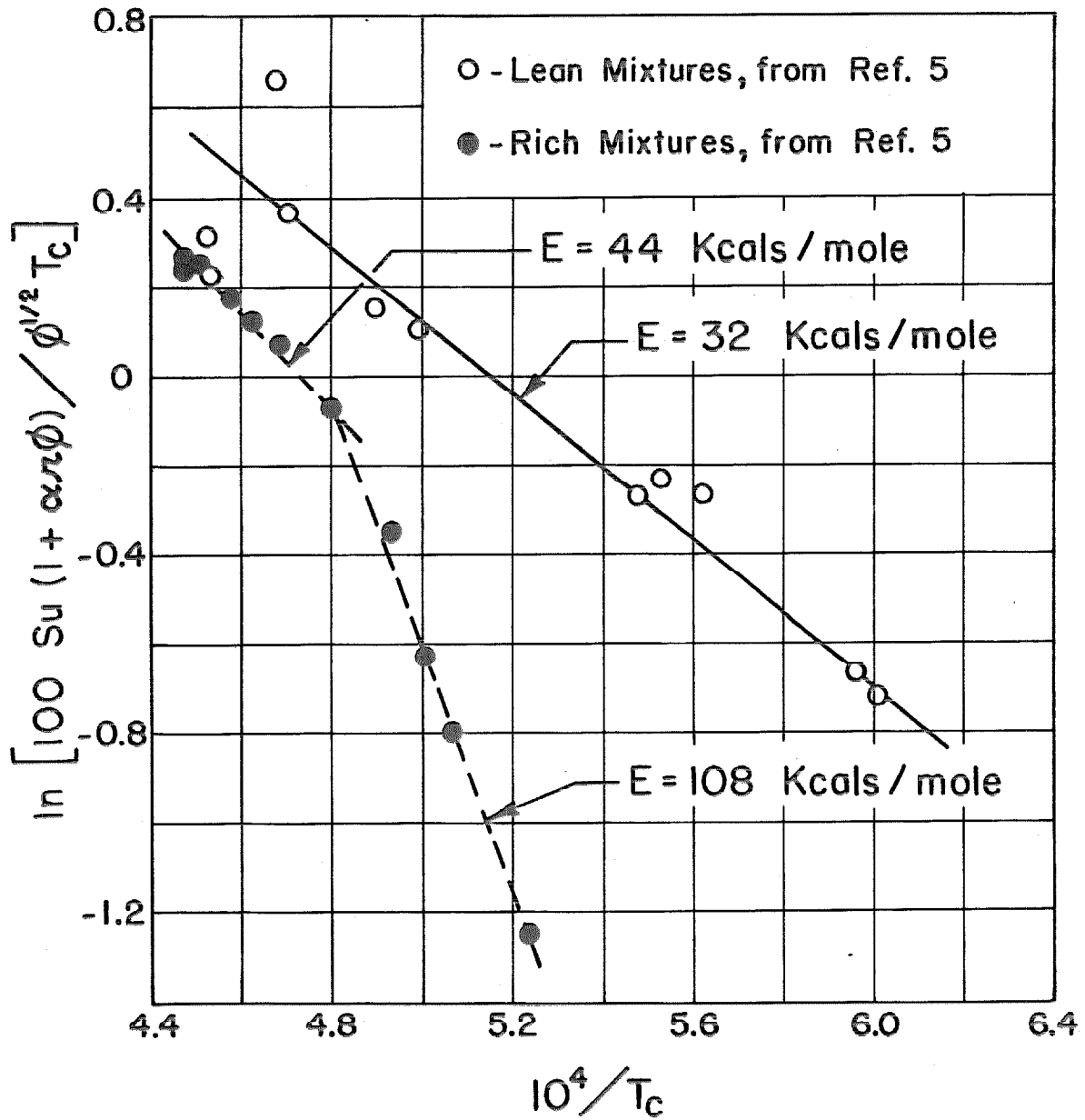


FIGURE 5. PLOT OF $\ln [100 S_u (1 + \alpha \pi \phi) / \phi^{1/2} T_c]$ vs $10^4 / T_c$ FOR METHANE - AIR FLAMES ($p=1$ ATMOS., $T_i =$ ROOM TEMPERATURE, DATA FROM REF. 5)

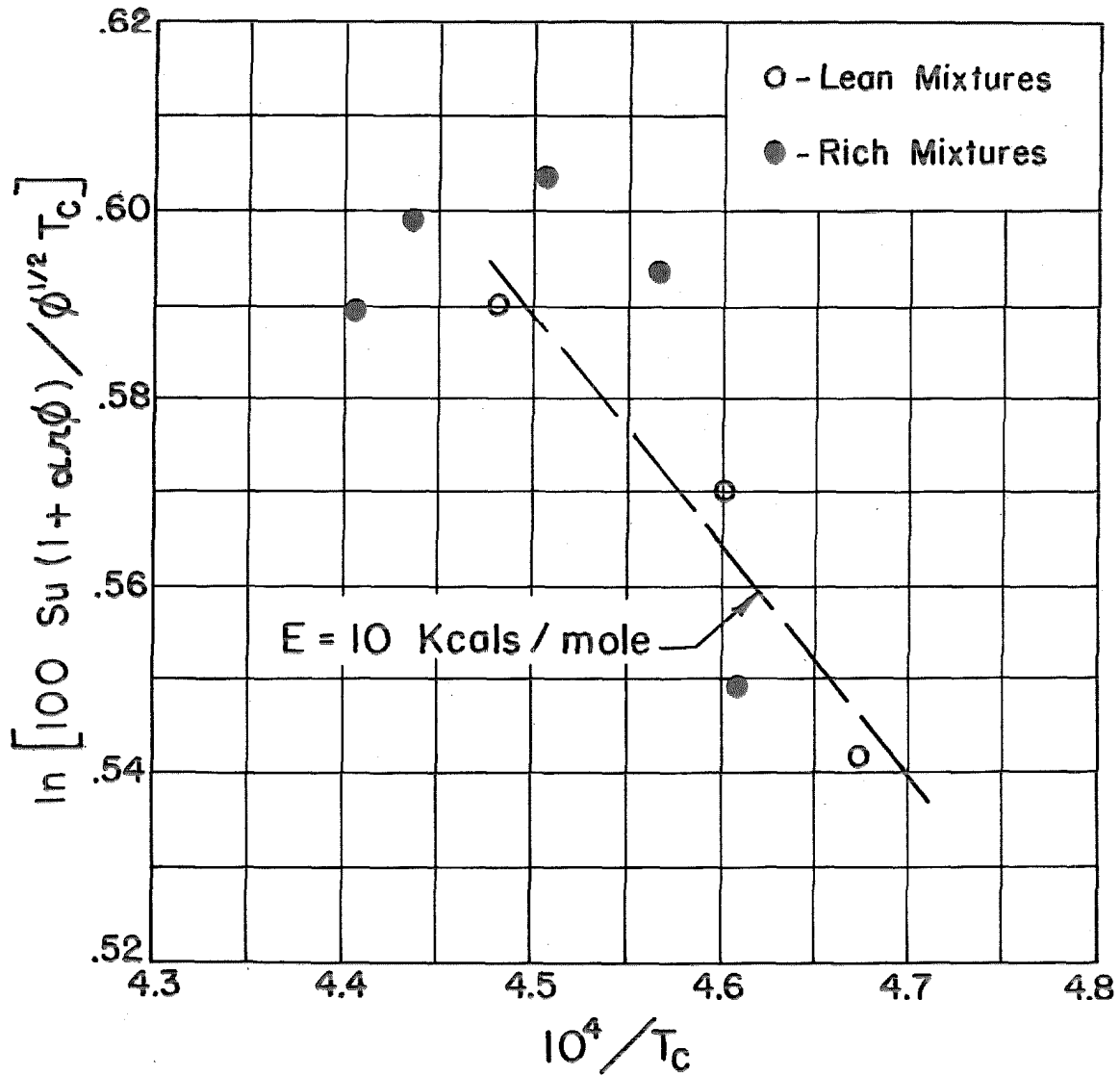


FIGURE 6. PLOT OF $\ln [100 S_u (1 + \alpha_L \phi) / \phi^{1/2} T_c]$ vs $10^4 / T_c$ FOR ETHANE - AIR FLAMES ($p=1$ ATMOS., $T_i =$ ROOM TEMPERATURE, DATA FROM REF. II)

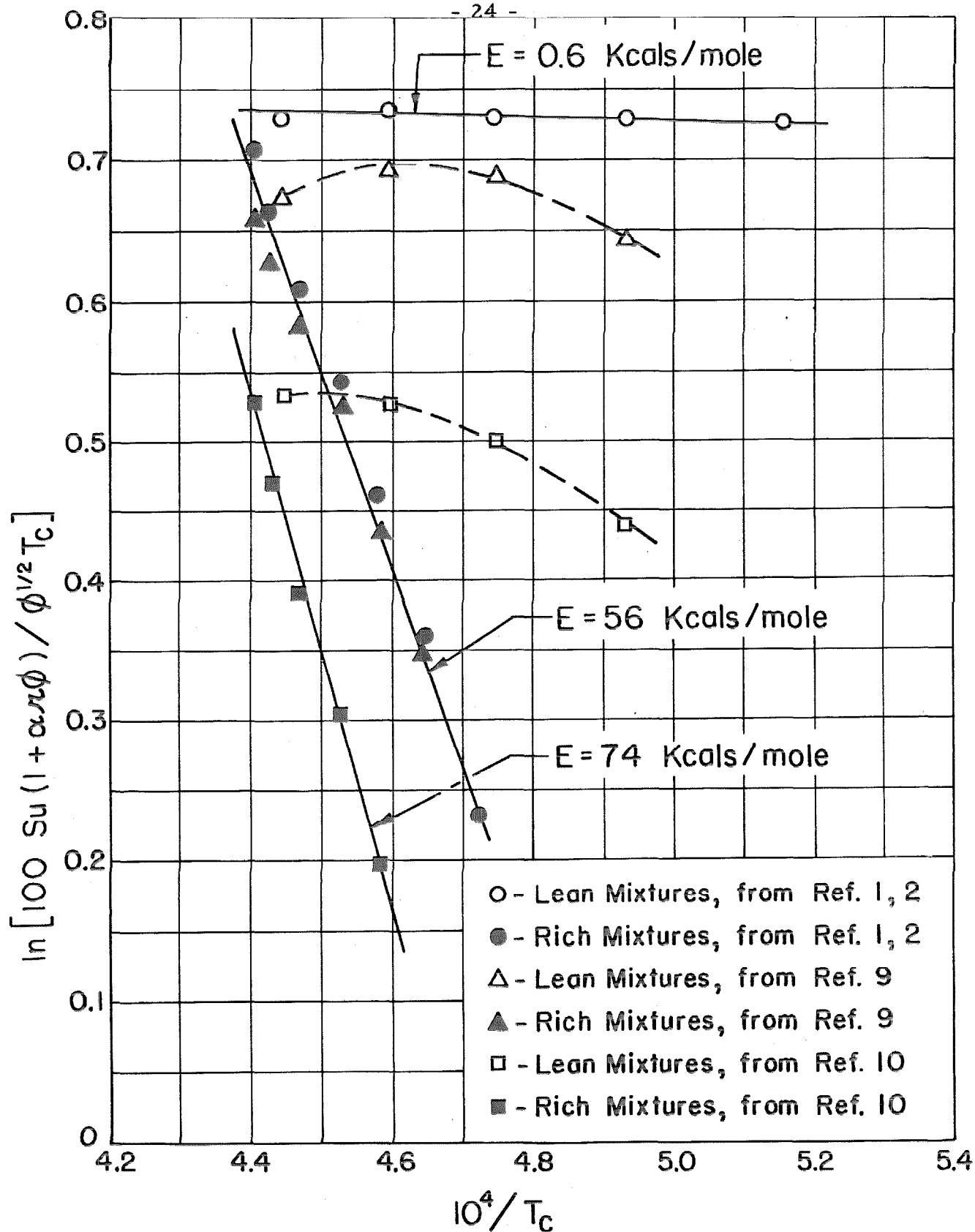


FIGURE 7. PLOT OF $\ln [100 S_u (1 + \alpha_n \phi) / \phi^{1/2} T_c]$ vs $10^4 / T_c$ FOR PROPANE-AIR FLAMES ($p = 1$ ATMOS., $T_i =$ ROOM TEMPERATURE)

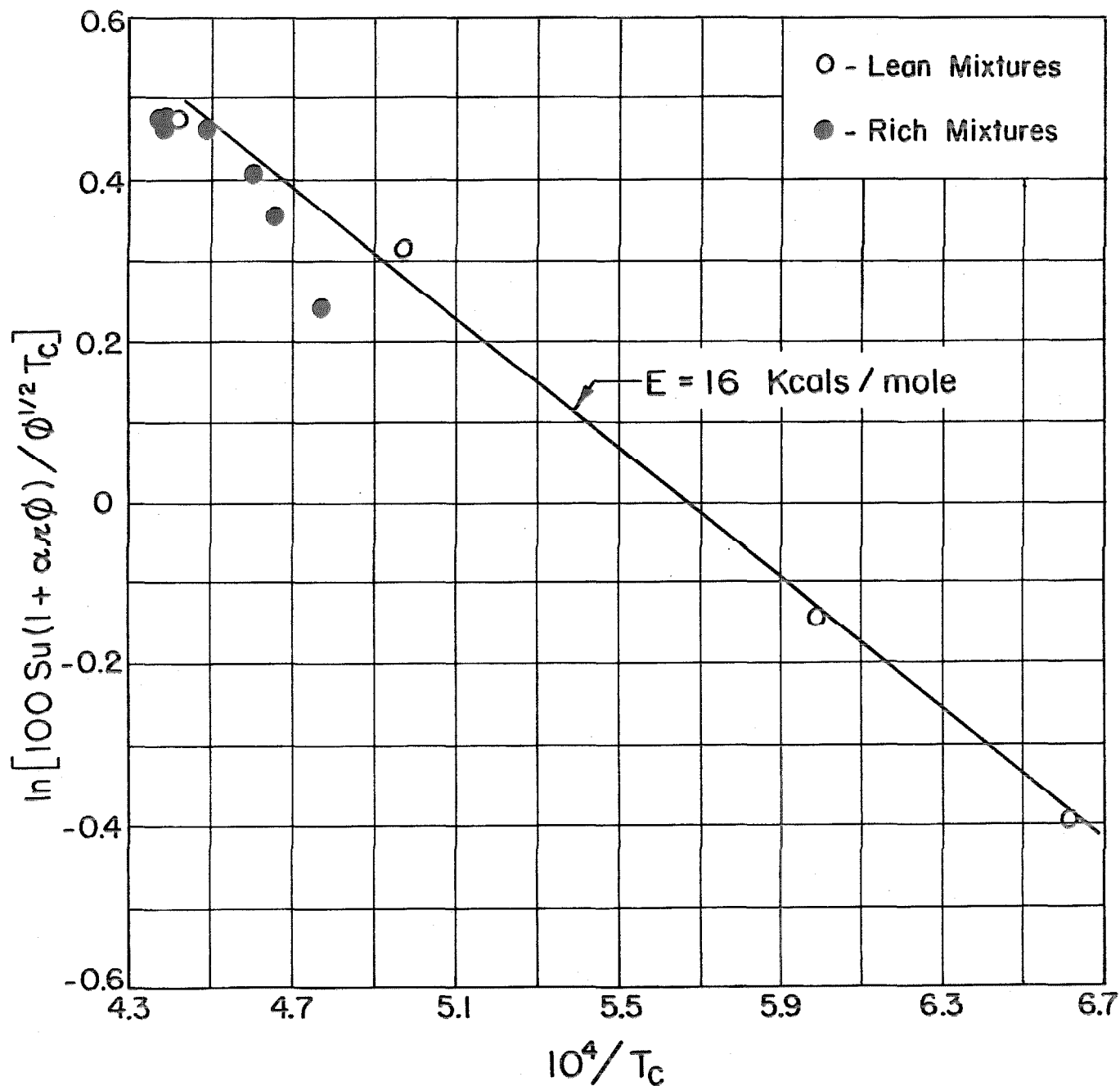
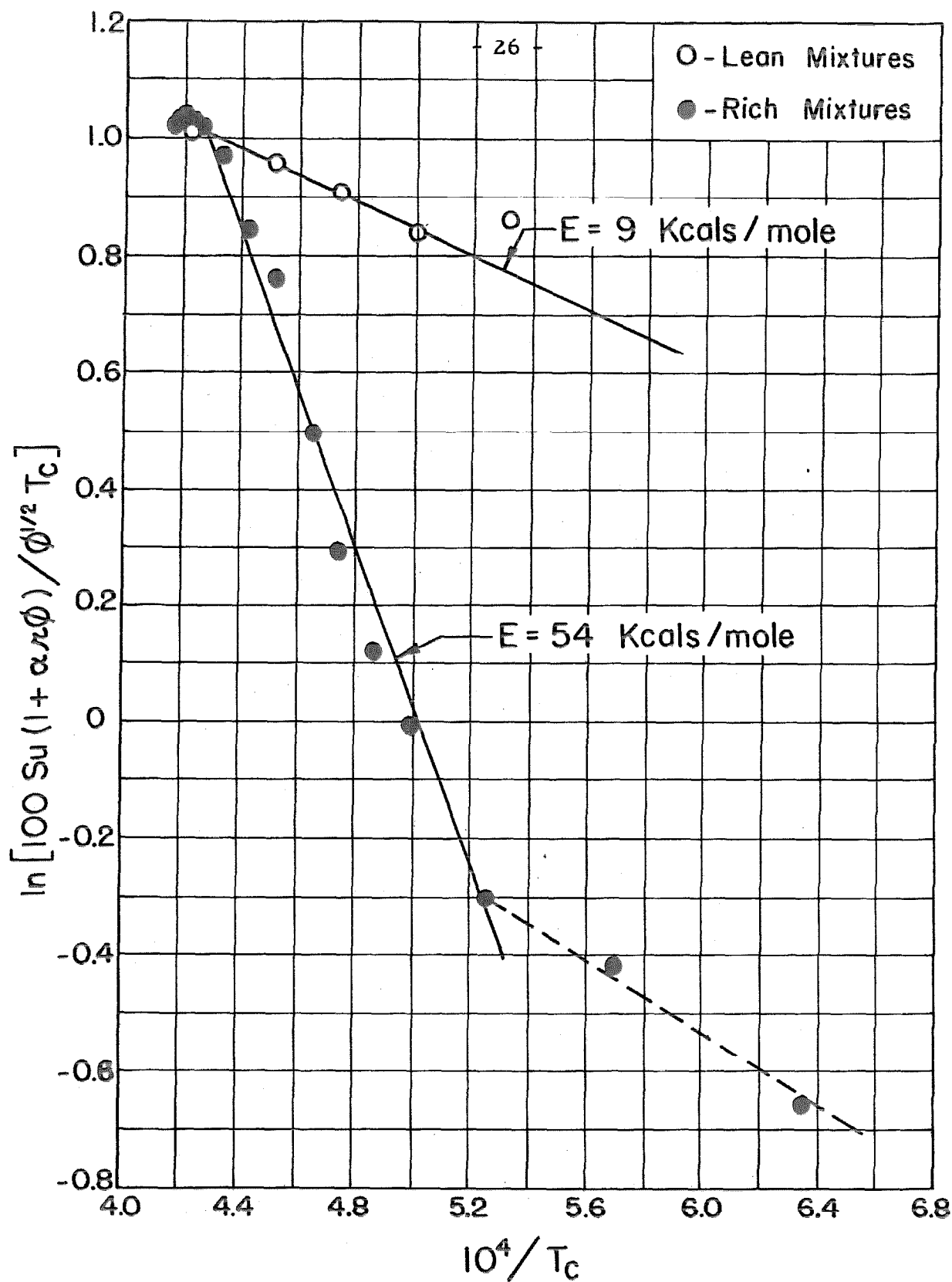


FIGURE 8. PLOT OF $\ln[100 Su(1 + \alpha_r \phi) / \phi^{1/2} T_c]$ vs $10^4 / T_c$ FOR PENTANE-AIR FLAMES. ($p=1$ ATMOS., T_i = ROOM TEMPERATURE, DATA FROM REF. 18)



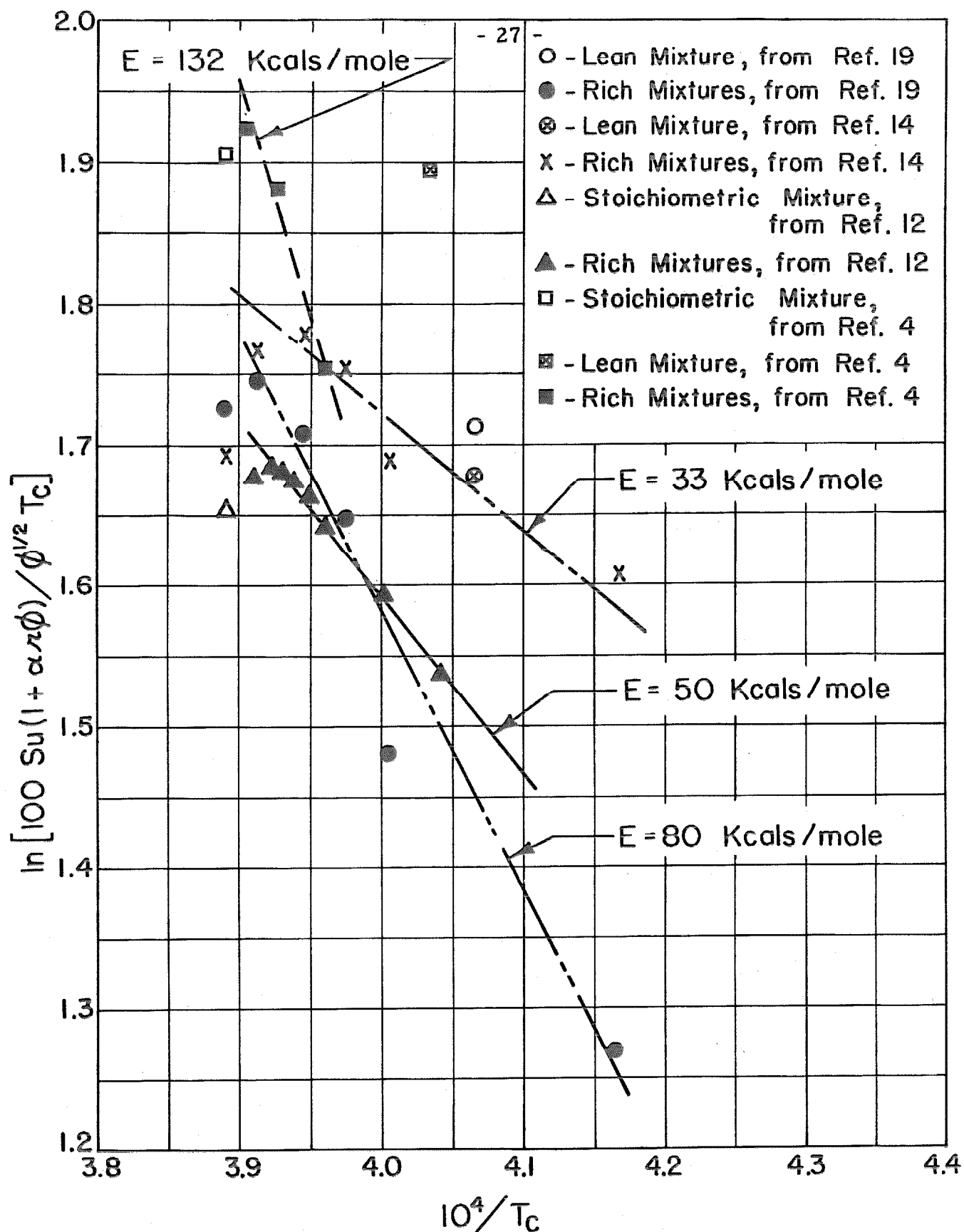


FIGURE 10. PLOT OF $\ln [100 Su(1 + \alpha \pi \phi) / \phi^{1/2} T_c]$ vs $10^4 / T_c$ FOR ACETYLENE - AIR FLAMES. ($p=1$ ATMOS., T_i = ROOM TEMPERATURE)

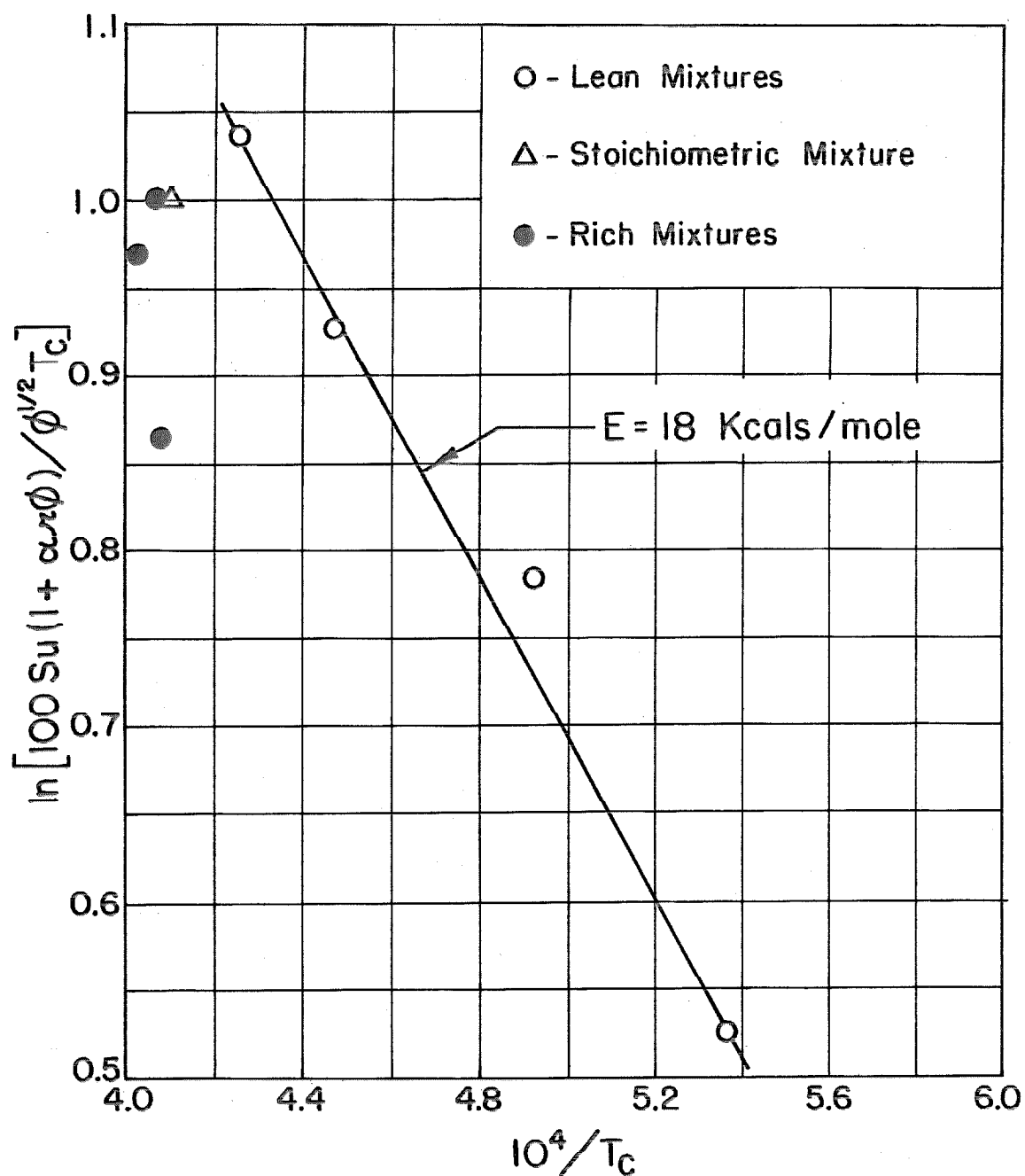


FIGURE 11. PLOT OF $\ln[100 Su(1 + \alpha_L \phi) / \phi^{1/2} T_c]$ vs $10^4 / T_c$ FOR PROPYNE - AIR FLAMES. ($p = 1 \text{ ATMOS.}$, $T_i = \text{ROOM TEMPERATURE}$, DATA FROM REF. 18)

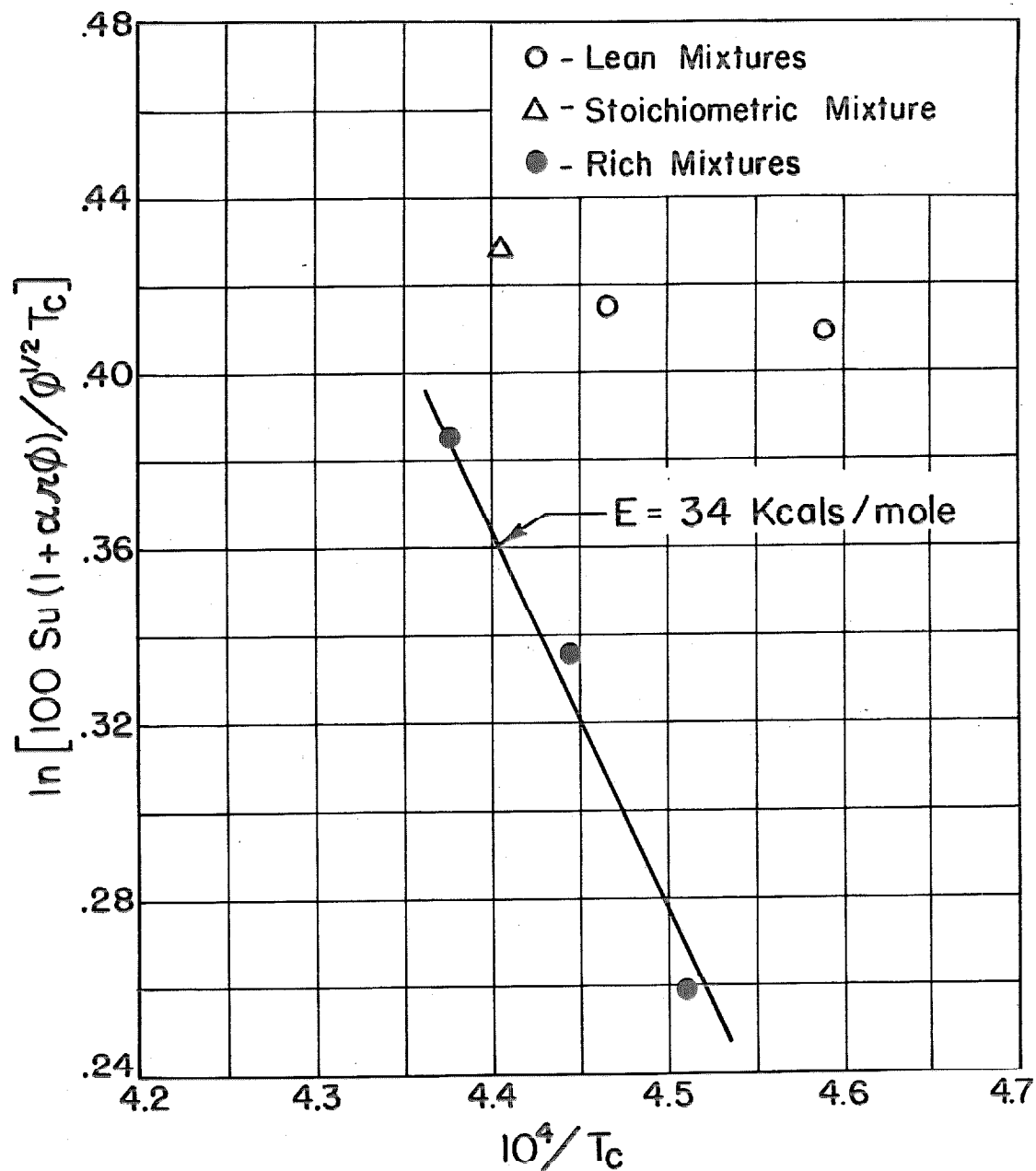


FIGURE 12. PLOT OF $\ln [100 S_u (1 + \alpha \pi \phi) / \phi^{1/2} T_c]$ vs $10^4 / T_c$ FOR 2,2,4-TRIMETHYL PENTANE-AIR FLAMES ($p=1$ ATMOS, $T_i=311^\circ\text{K}$, DATA FROM REF.8)

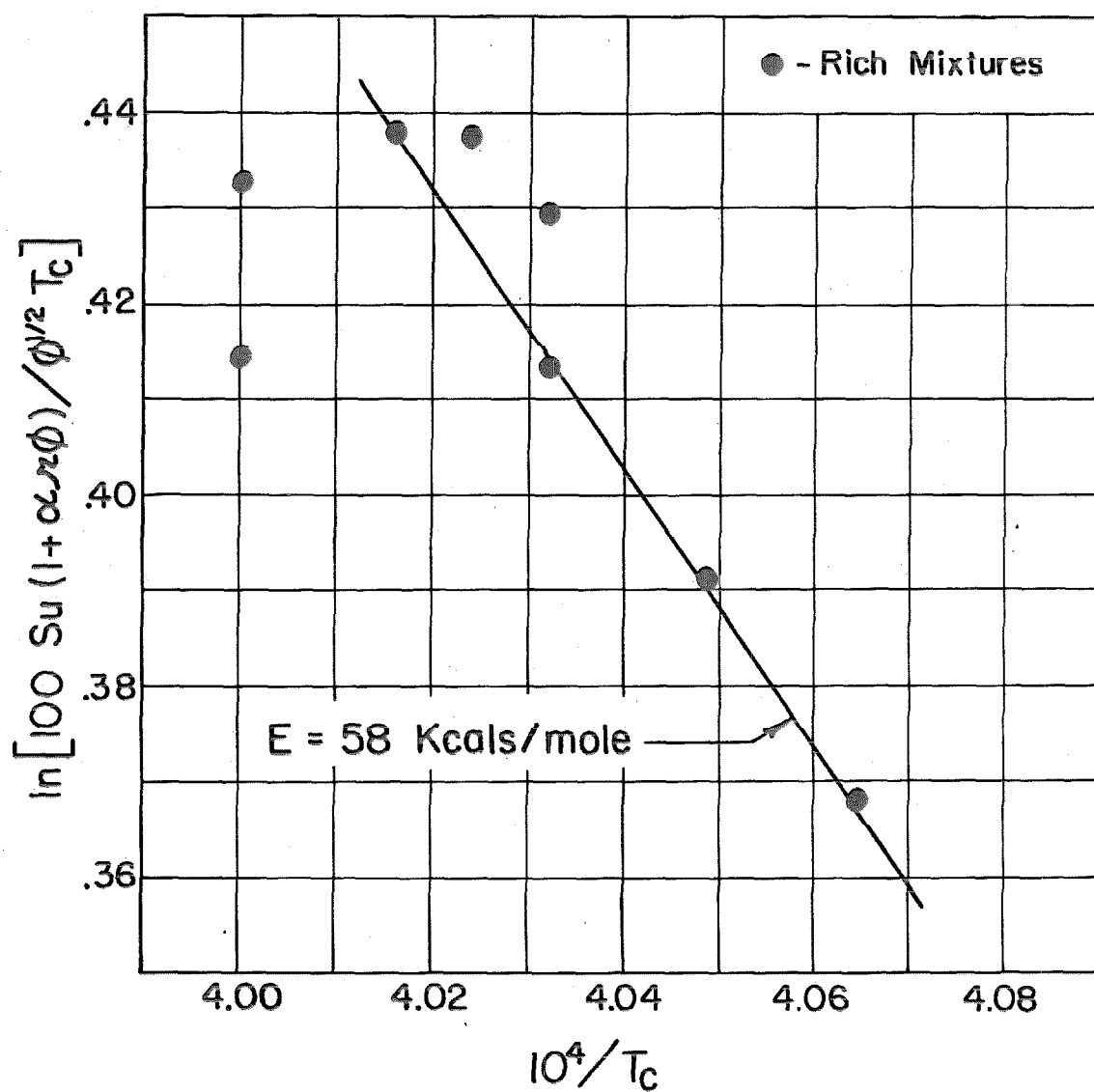
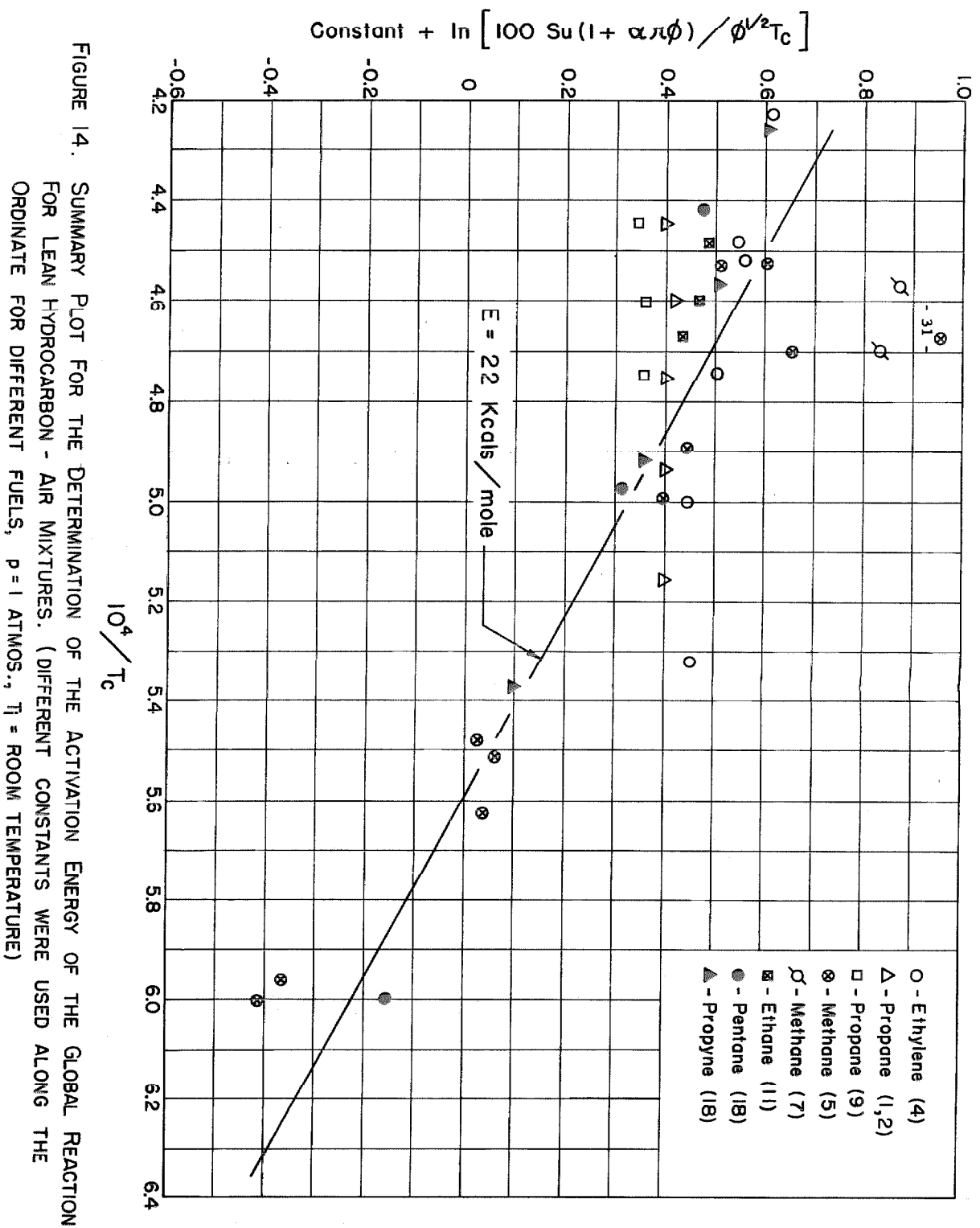


FIGURE 13. PLOT OF $\ln[100 S_u (1 + \alpha_L \phi) / \phi^{1/2} T_c]$ vs $10^4 / T_c$ FOR BENZENE - AIR FLAMES. ($p = 1$ ATMOS., $T_i =$ ROOM TEMPERATURE, DATA FROM REF. 11)



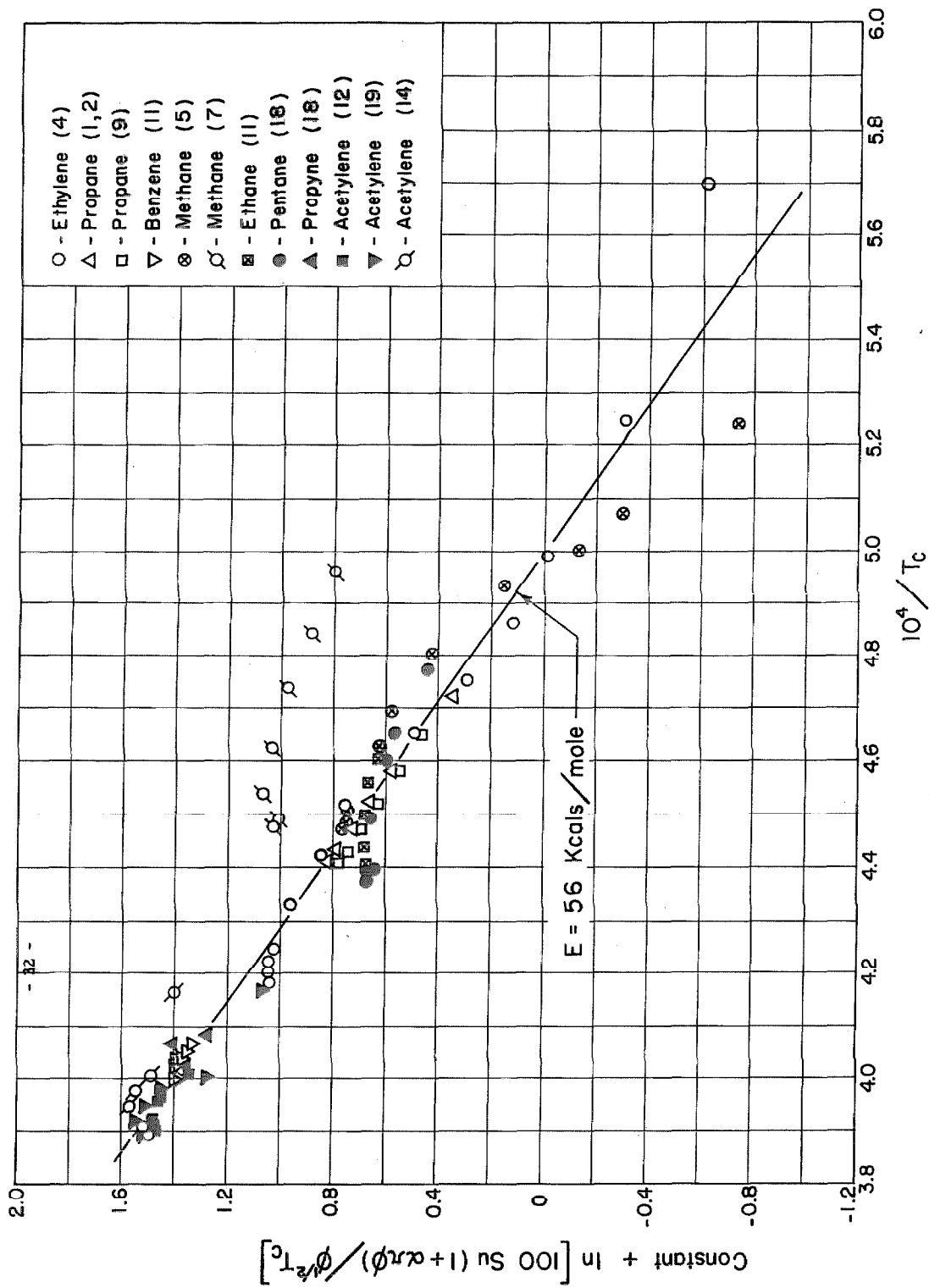


FIGURE 15. SUMMARY PLOT FOR THE DETERMINATION OF THE ACTIVATION ENERGY OF THE GLOBAL REACTION FOR RICH HYDROCARBON-AIR MIXTURES. (DIFFERENT CONSTANTS WERE USED ALONG THE ORDINATE FOR DIFFERENT FUELS, $p = 1 \text{ ATMOS.}$, $T_r = \text{ROOM TEMPERATURE}$)

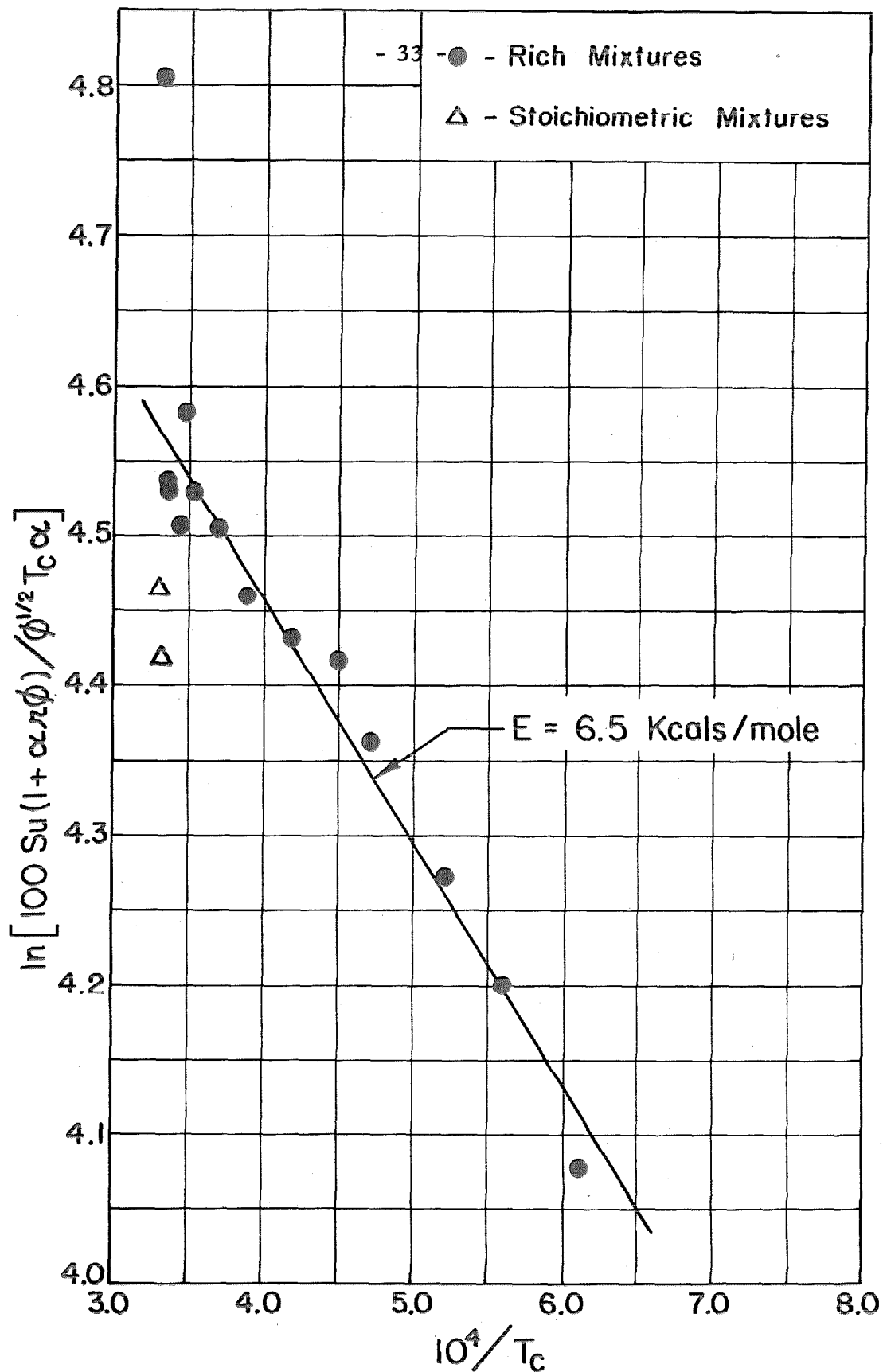


FIGURE 16. PLOT OF $\ln[100 Su(1 + \alpha n \phi) / \phi^{1/2} T_c \alpha]$ vs $10^4 / T_c$ FOR $H_2 - O_2 - N_2$ FLAMES. ($p = 1 \text{ ATMOS.}$, $T_i = \text{ROOM TEMPERATURE}$, DATA FROM REF. 16)

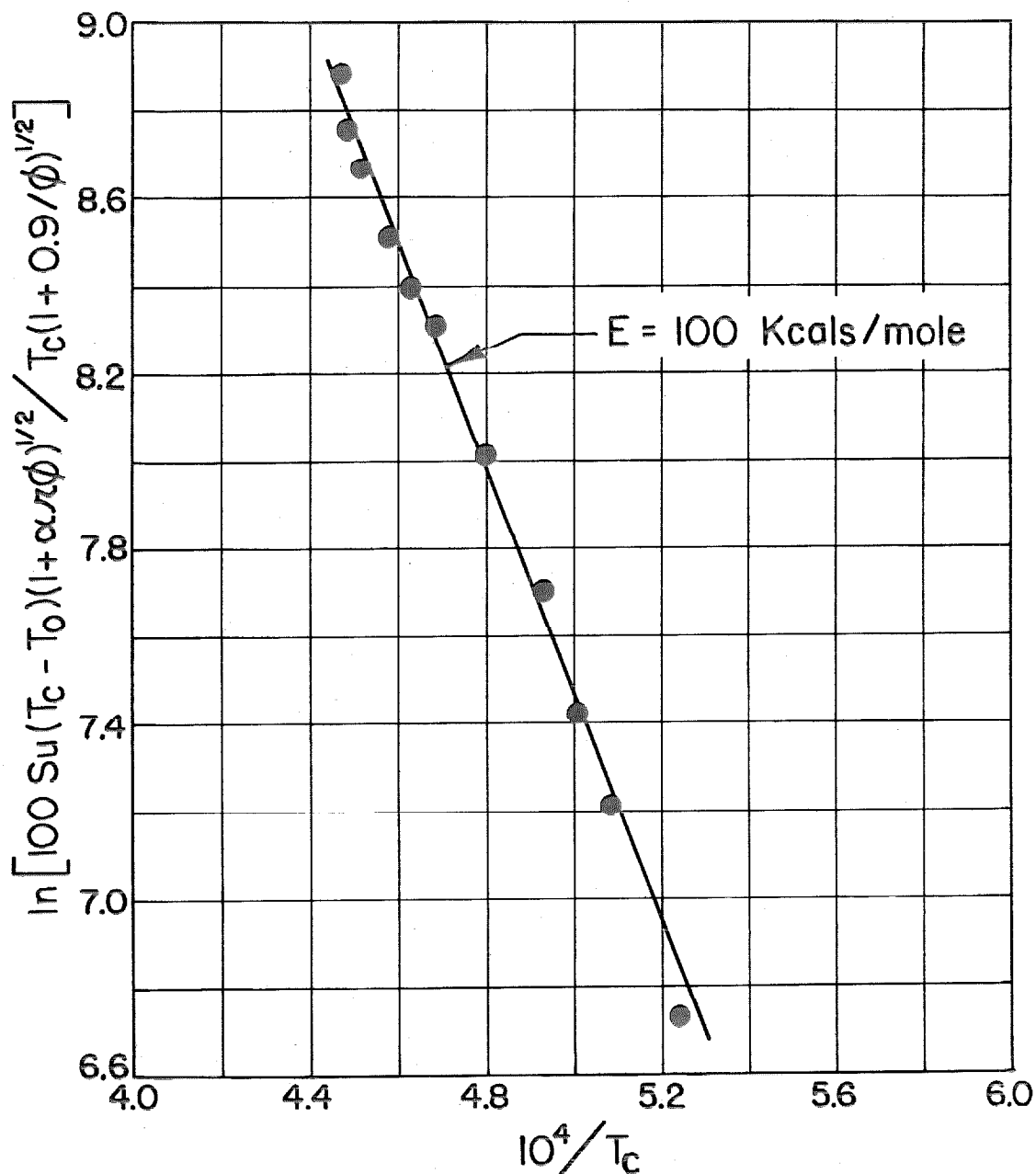


FIGURE 17. PLOT OF $\ln \left[\frac{100 S_u (T_c - T_0) (1 + \alpha \phi)^{1/2}}{T_c (1 + 0.9/\phi)^{1/2}} \right]$ vs $10^4 / T_c$ FOR METHANE-AIR FLAMES.
($p = 1$ ATMOS., $T_i =$ ROOM TEMPERATURE, DATA FROM REF. 5)

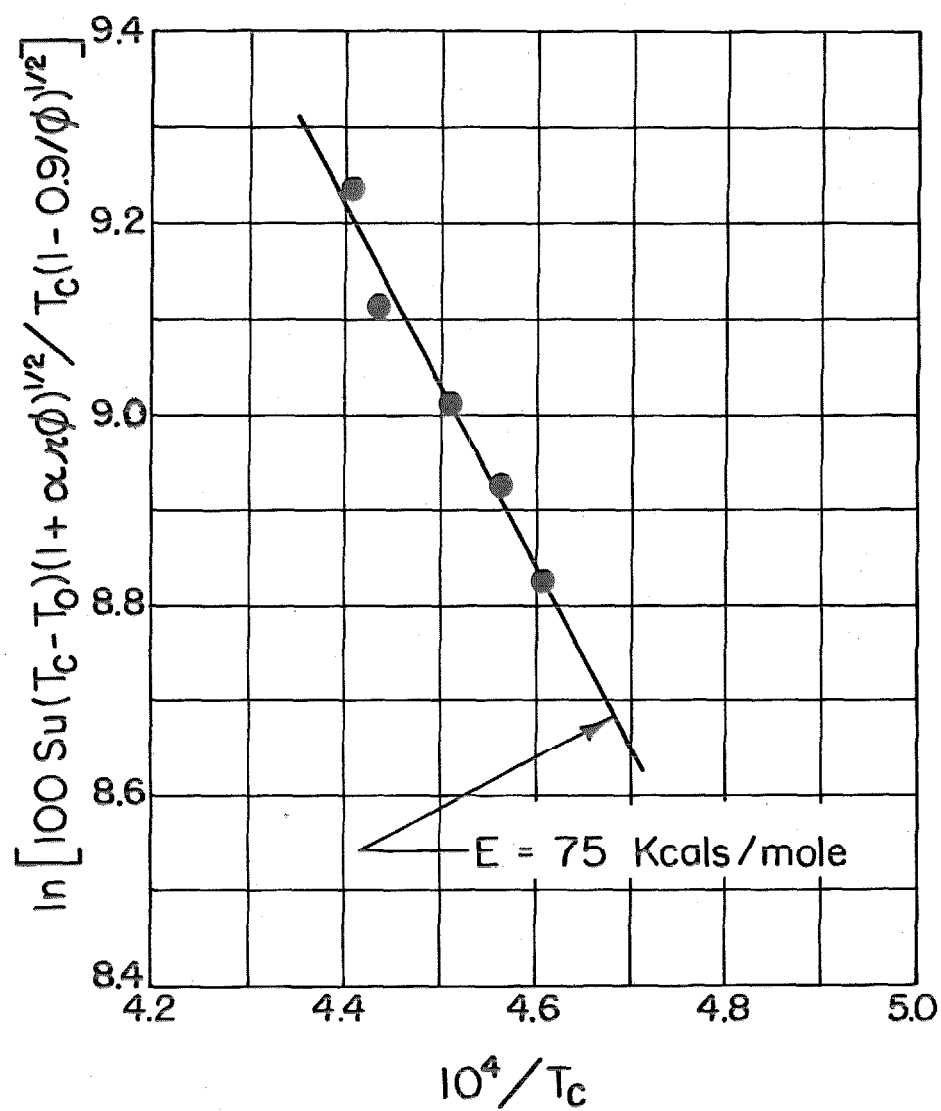


FIGURE 18. PLOT OF $\ln \left[\frac{100 S_u (T_c - T_0) (1 + \alpha_r \phi)^{1/2}}{T_c (1 - 0.9/\phi)^{1/2}} \right]$ vs $10^4/T$ FOR ETHANE-AIR FLAMES. ($p = 1$ ATMOS., $T_i =$ ROOM TEMPERATURE, DATA FROM REF. 10)

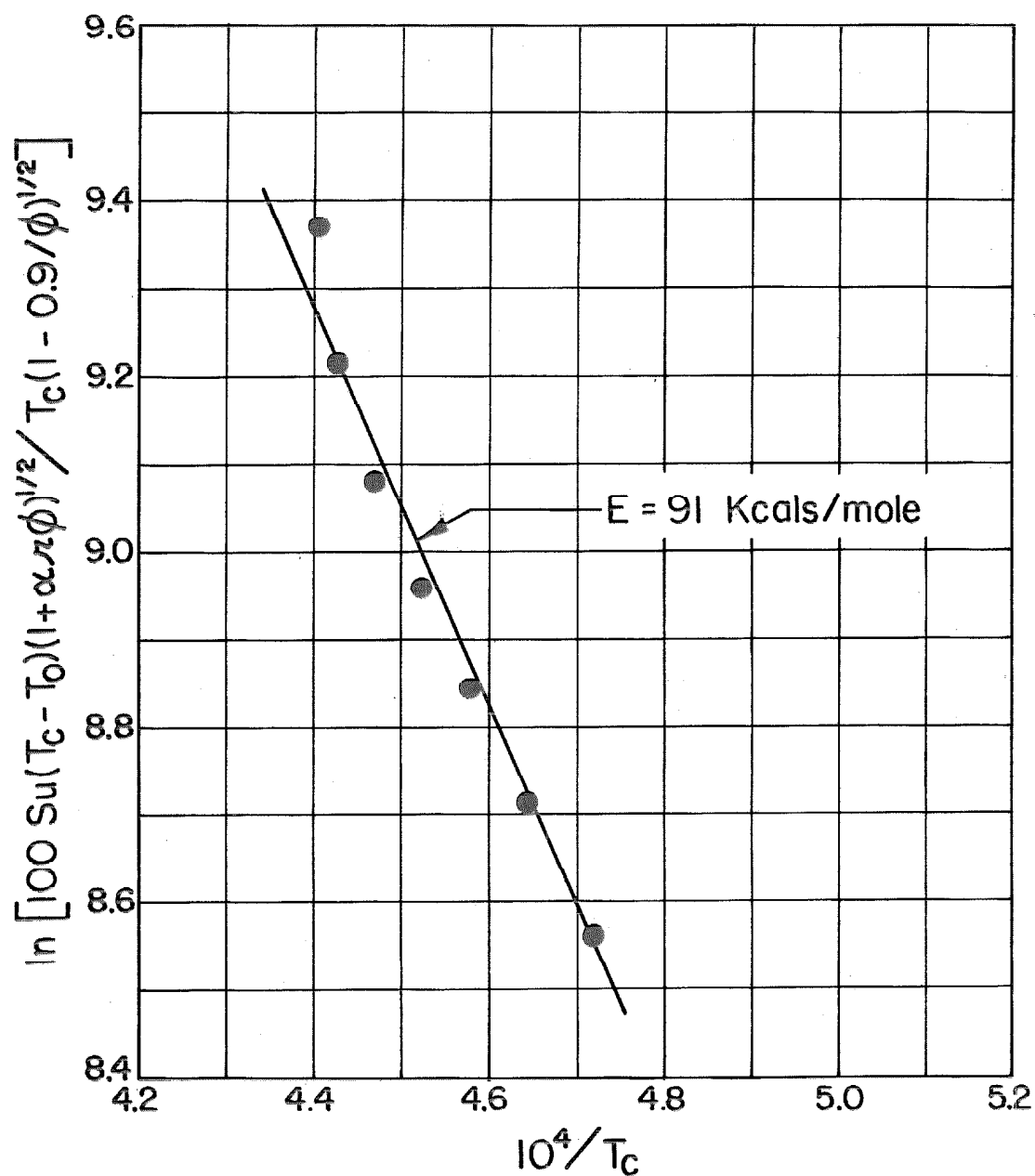


FIGURE 19. PLOT OF $\ln \left[\frac{100 S_u (T_c - T_0) (1 + \alpha \pi \phi)^{1/2}}{T_c (1 - 0.9/\phi)^{1/2}} \right]$ vs $10^4 / T_c$ FOR PROPANE-AIR FLAMES.
 ($p = 1$ ATMOS., $T_i =$ ROOM TEMPERATURE, DATA FROM REF. 1,2)

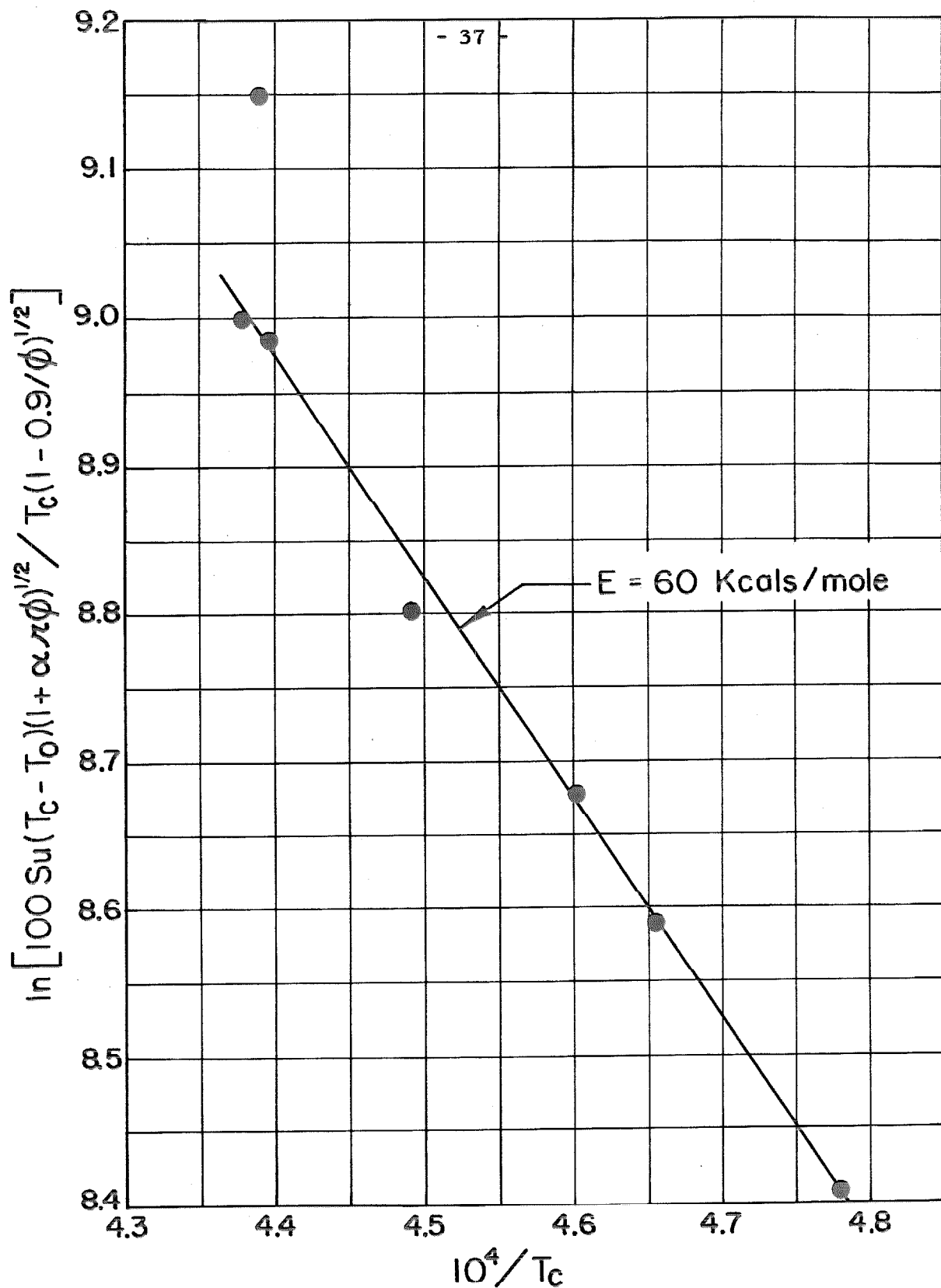


FIGURE 20. PLOT OF $\ln \left[\frac{100 S_u (T_c - T_0) (1 + \alpha \phi)^{1/2}}{T_c (1 - 0.9/\phi)^{1/2}} \right]$ vs $10^4 / T_c$ FOR PENTANE - AIR FLAMES.
 ($p = 1 \text{ ATMOS.}$, $T_i = \text{ROOM TEMPERATURE}$, DATA FROM REF. 20)

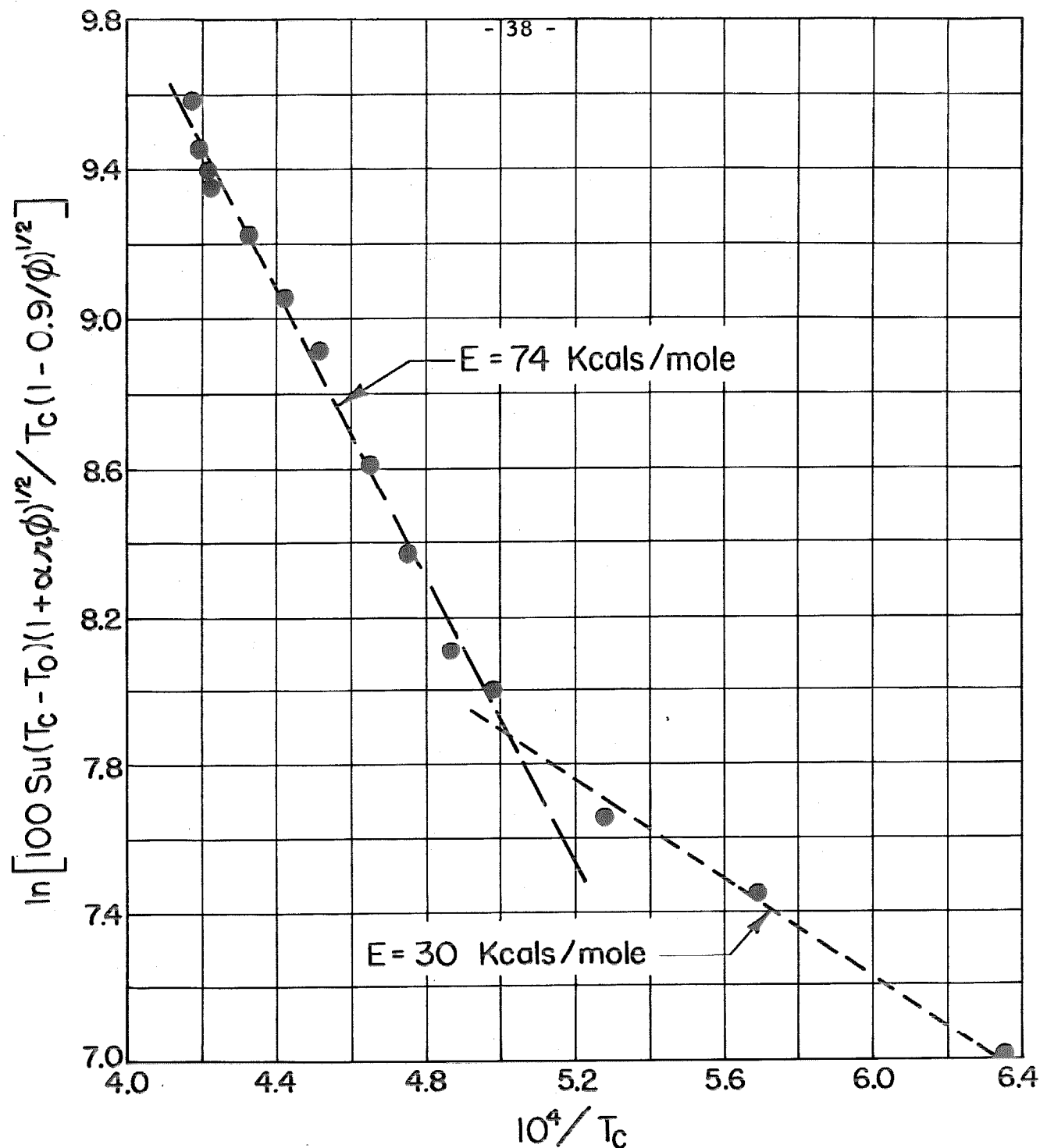


FIGURE 21. PLOT OF $\ln \left[100 Su (T_c - T_0) (1 + \alpha \pi \phi)^{1/2} / T_c (1 - 0.9/\phi)^{1/2} \right]$ vs $10^4 / T_c$ FOR ETHYLENE-AIR FLAMES.
 ($p = 1 \text{ ATMOS.}$, $T_i = \text{ROOM TEMPERATURE}$, DATA FROM REF. 20)

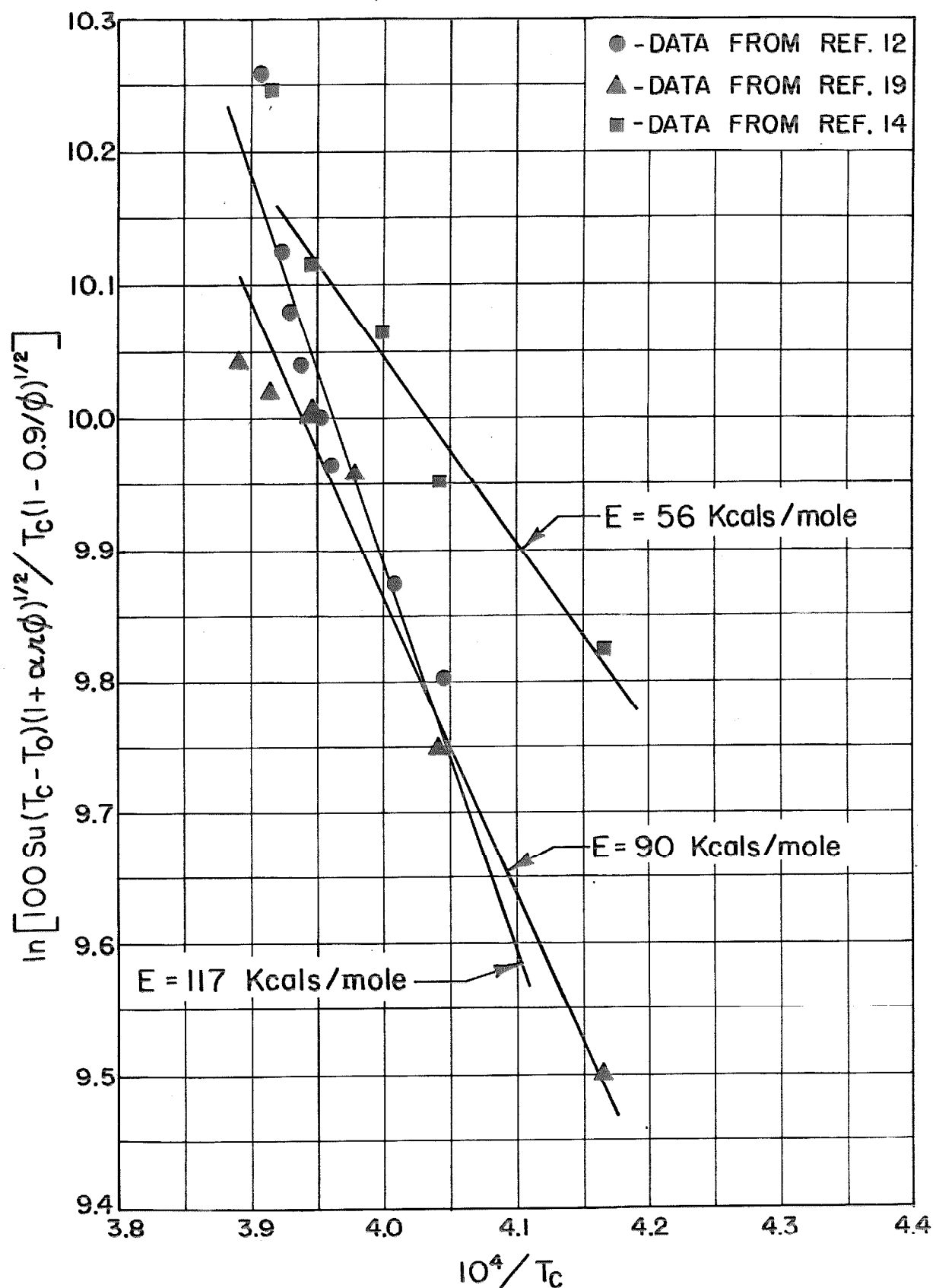


FIGURE 22. PLOT OF $\ln \left[100 S_u (T_c - T_0) (1 + \alpha \lambda \phi)^{1/2} / T_c (1 - 0.9/\phi)^{1/2} \right]$ vs $10^4 / T_c$ FOR ACETYLENE-AIR FLAMES. (p = 1 ATMOS., T_i = ROOM TEMPERATURE.)

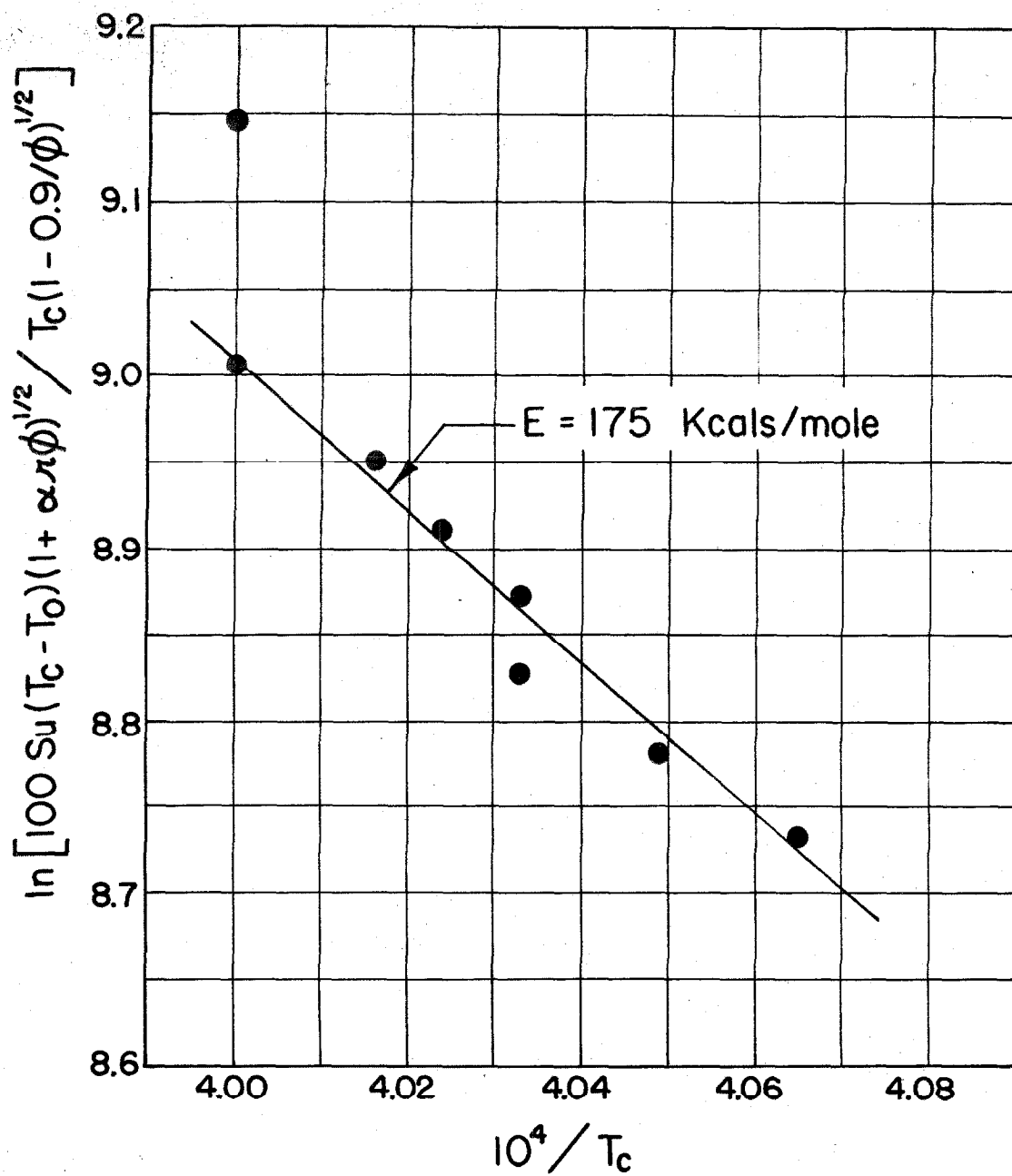


FIGURE 23. PLOT OF $\ln \left[\frac{100 S_u (T_c - T_0) (1 + \alpha \phi)^{1/2}}{T_c (1 - 0.9/\phi)^{1/2}} \right]$ vs $10^4 / T_c$ FOR BENZENE-AIR FLAMES.
($p = 1$ ATMOS., $T_i =$ ROOM TEMPERATURE, DATA FROM REF. 10)

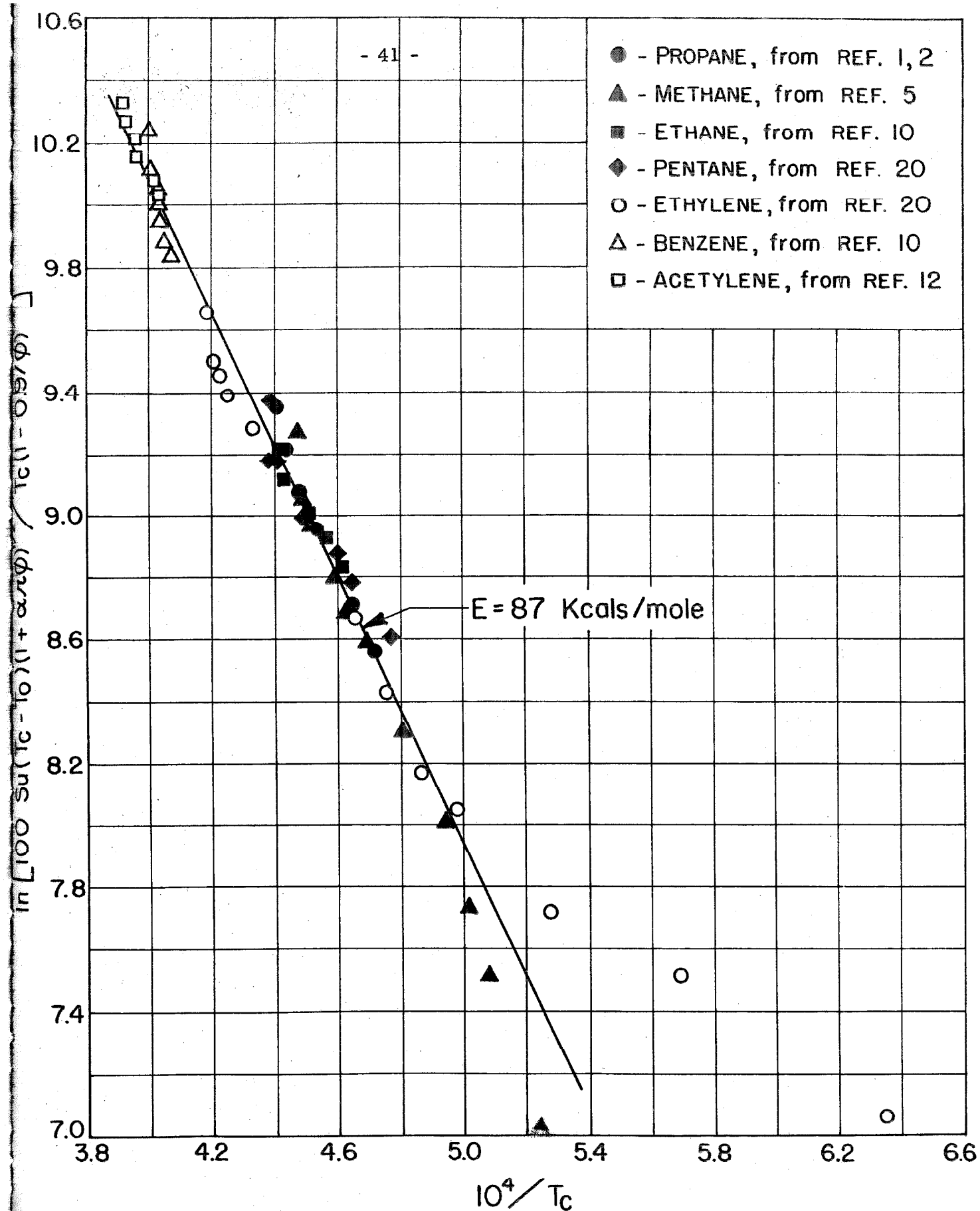


FIGURE 24. SUMMARY PLOT OF RICH HYDROCARBON - AIR FLAMES.
($p = 1 \text{ ATMOS.}$, $T_i = \text{ROOM TEMPERATURE}$)

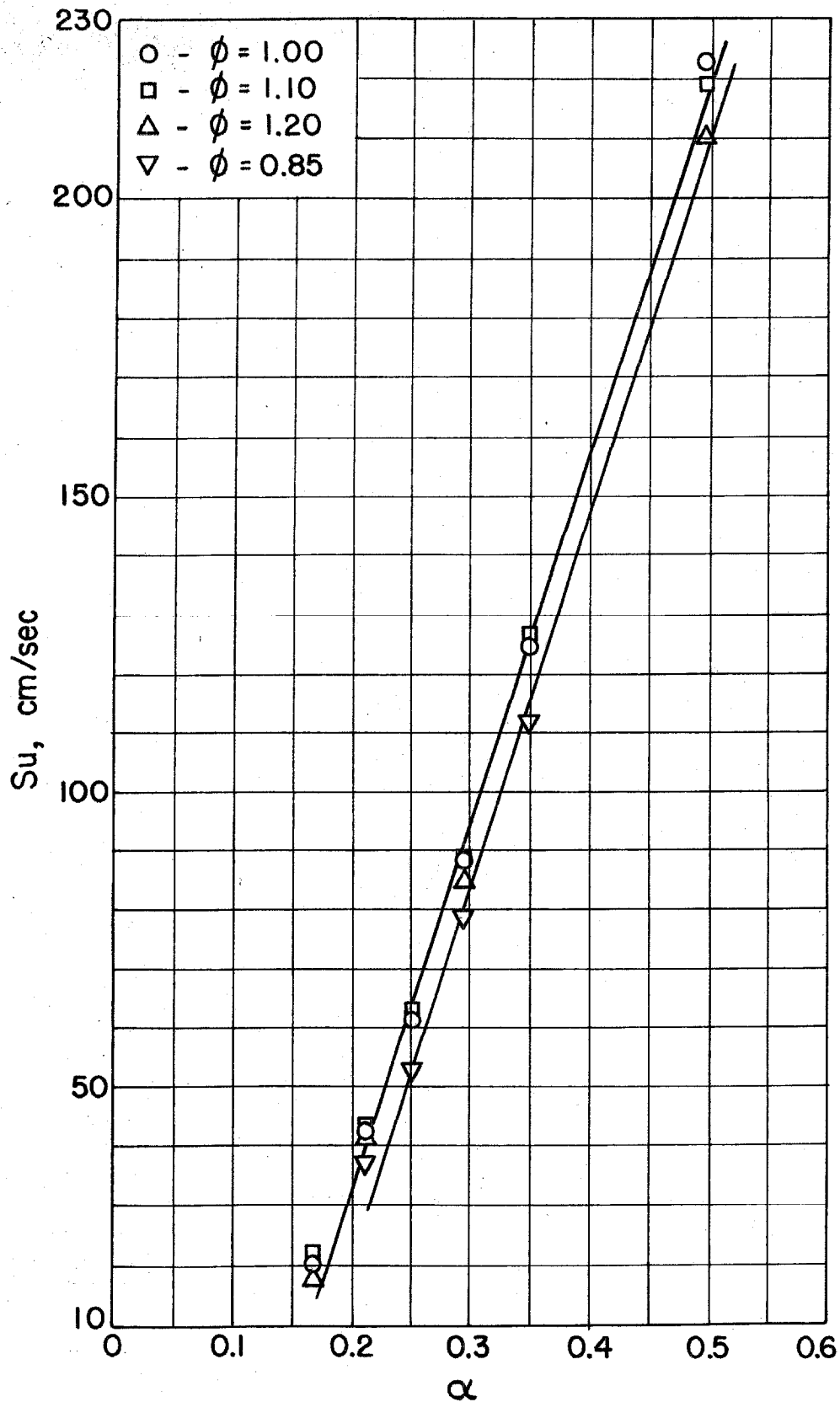


FIGURE 25. PLOT OF S_u vs α FOR PROPANE - OXYGEN - NITROGEN MIXTURES. ($p = 1$ ATMOS., $T_i = 311^\circ\text{K}$, DATA FROM REF. 9)

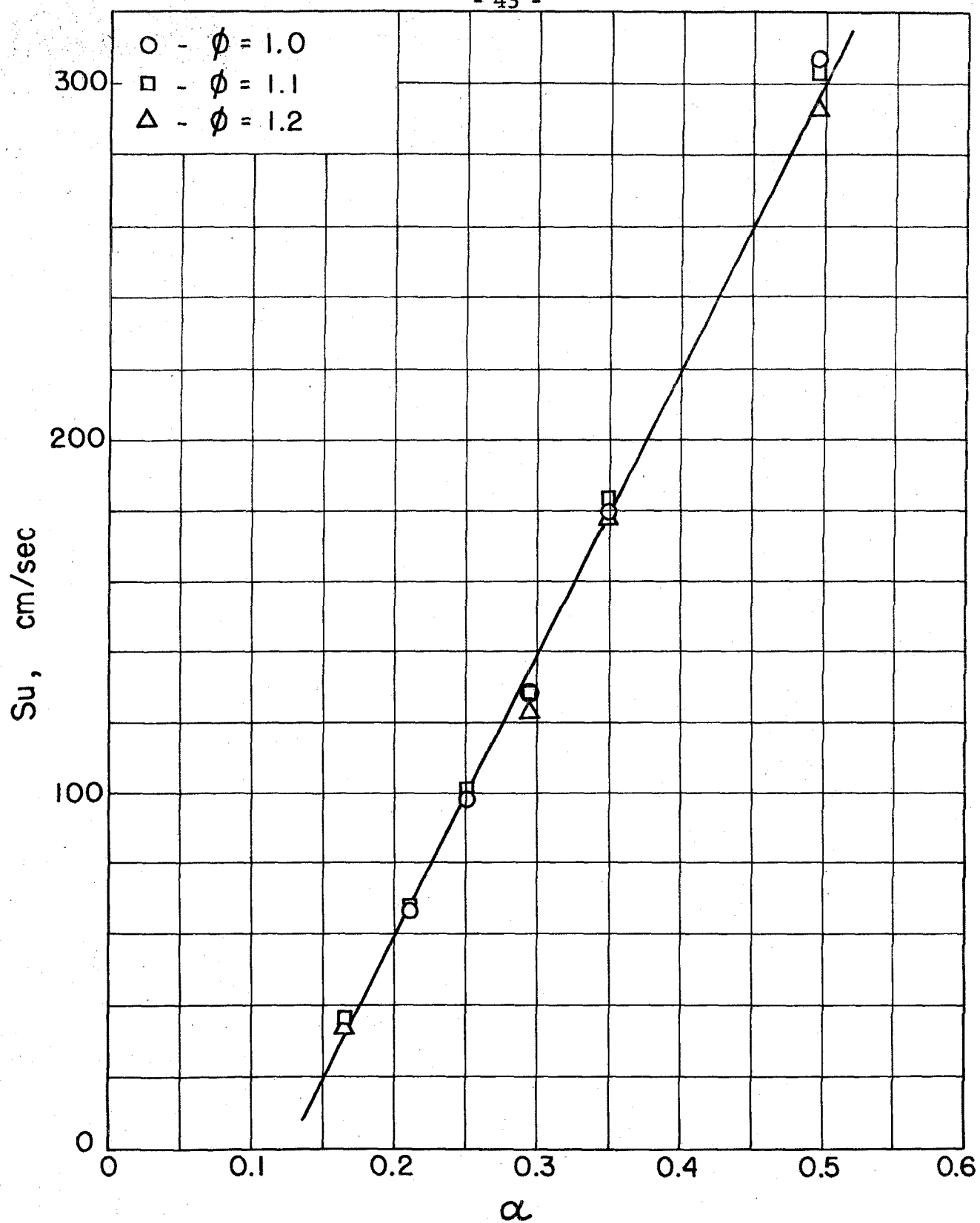


FIGURE 26. PLOT OF S_u vs α FOR PROPANE - OXYGEN - NITROGEN MIXTURES ($p = 1$ ATMOS., $T_i = 422$ °K, DATA FROM REF. 9)

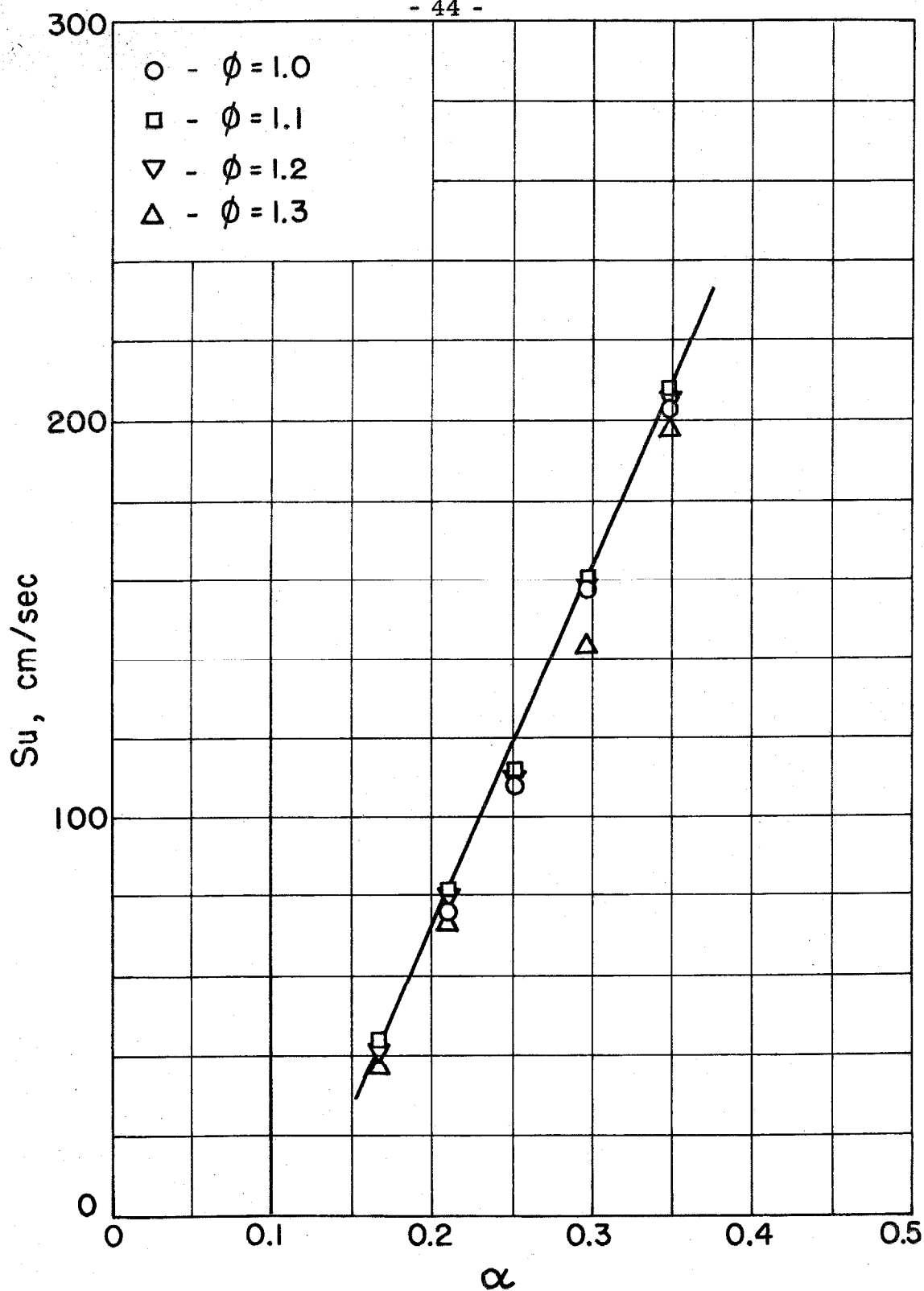


FIGURE 27. PLOT OF S_u vs α FOR ETHYLENE - OXYGEN - NITROGEN MIXTURES. ($p = 1$ ATMOS., $T_i = 311^\circ\text{K}$, DATA FROM REF. 9)

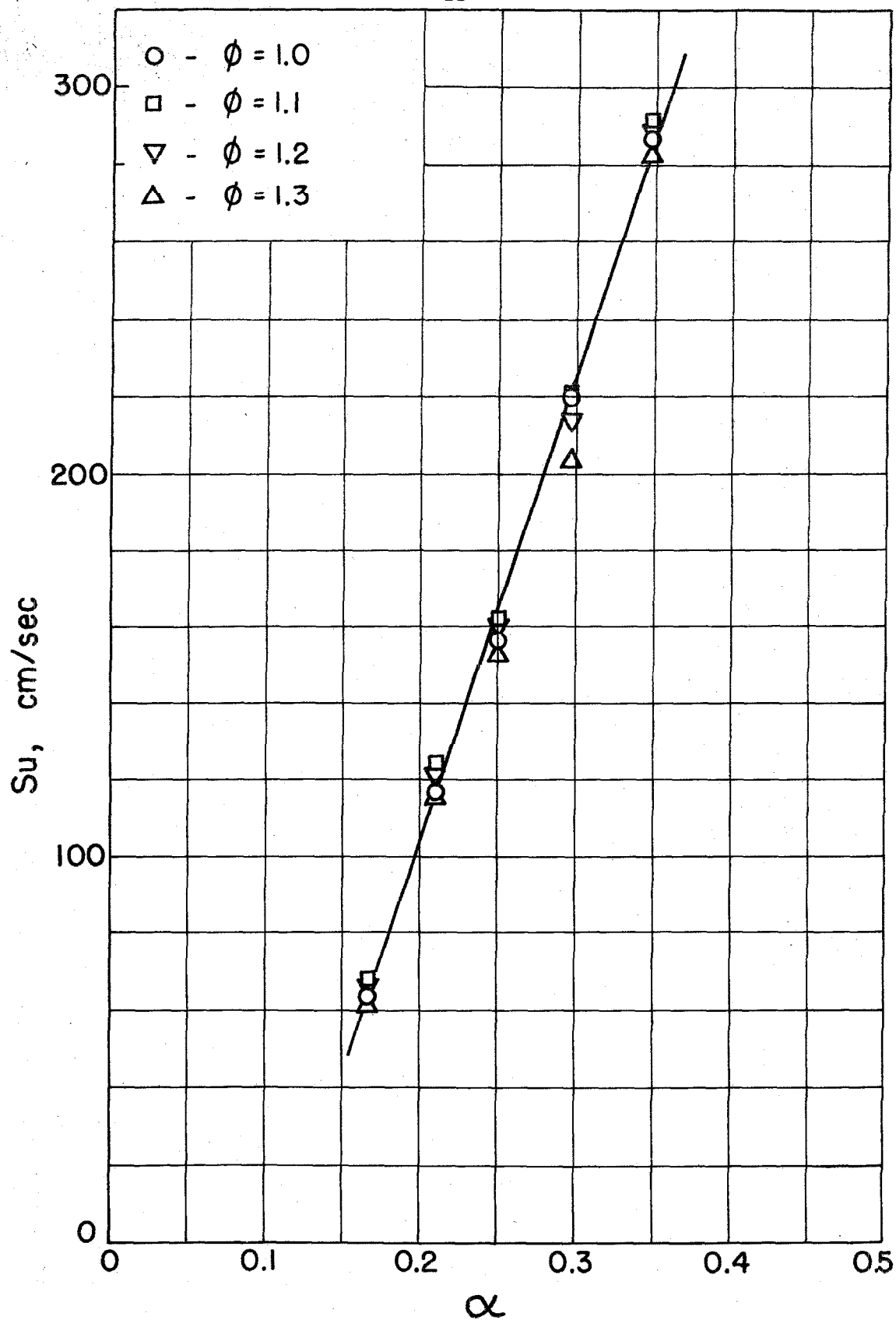


FIGURE 28. PLOT OF S_u vs α FOR ETHYLENE - OXYGEN - NITROGEN MIXTURES. ($p = 1$ ATMOS., $T_i = 422^\circ\text{K}$, DATA FROM REF. 9)

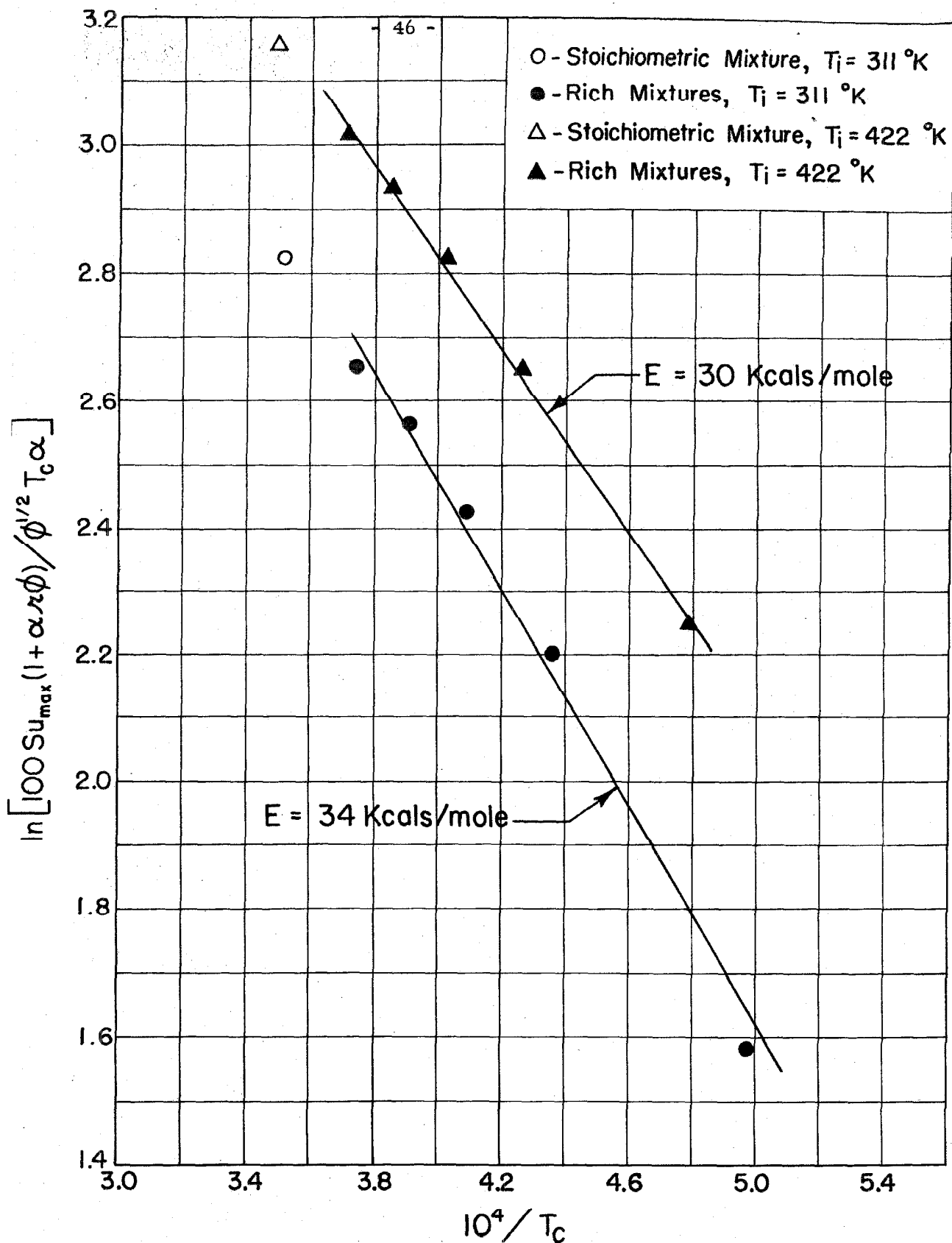


FIGURE 29. PLOT OF $\ln[100 S_{u_{\max}} (1 + \alpha r \phi) / \phi^{1/2} T_c \alpha]$ vs $10^4 / T_c$ FOR PROPANE - O_2 - N_2 FLAMES.

($p = 1$ ATMOS., DATA FROM REF. 9)

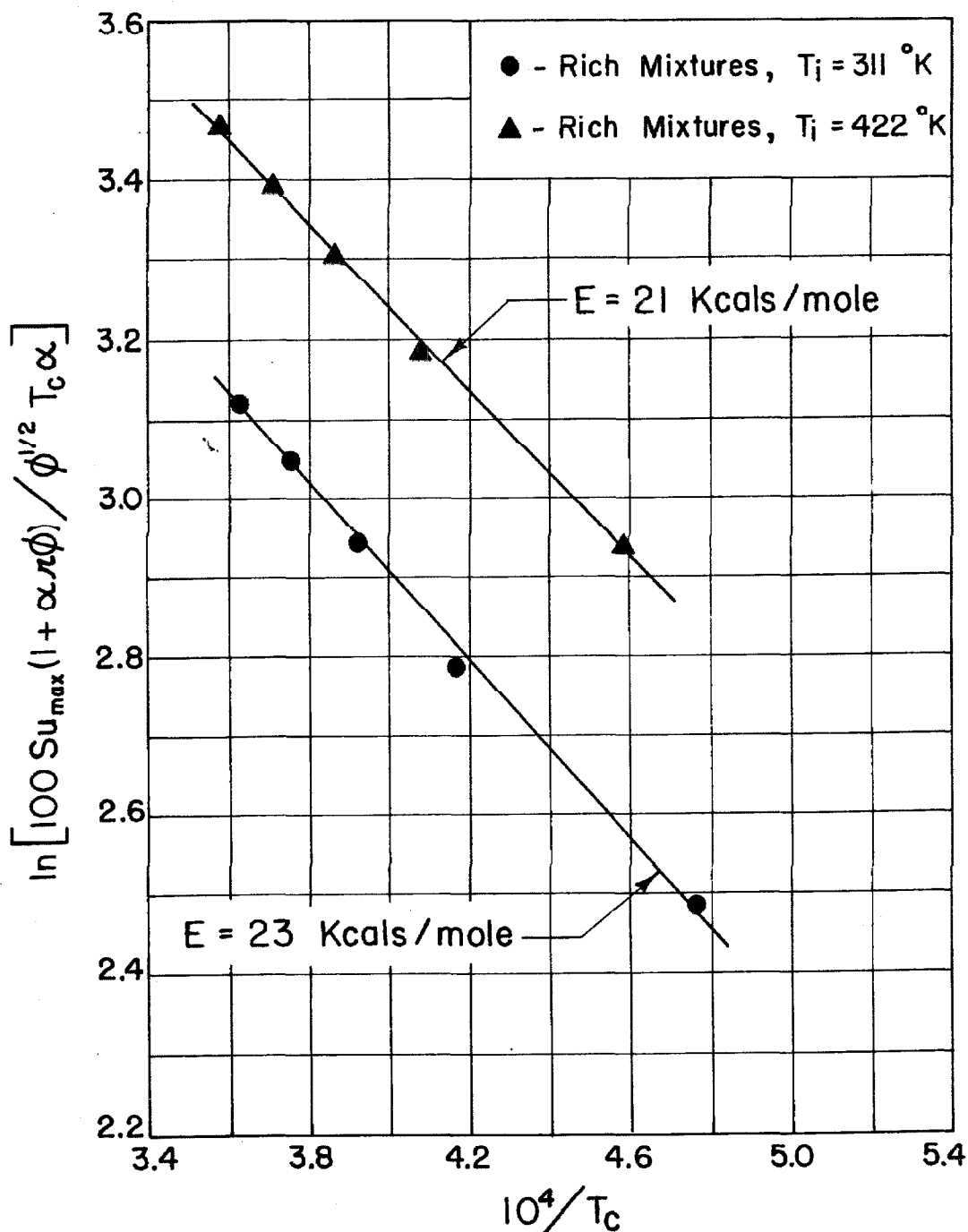


FIGURE 30. PLOT OF $\ln[100 S_{u_{\max}}(1 + \alpha \phi)/\phi^{1/2} T_c \alpha]$ vs $10^4/T_c$ FOR ETHYLENE- O_2 - N_2 FLAMES. ($p = 1 \text{ ATMOS.}$, DATA FROM REF. 9)

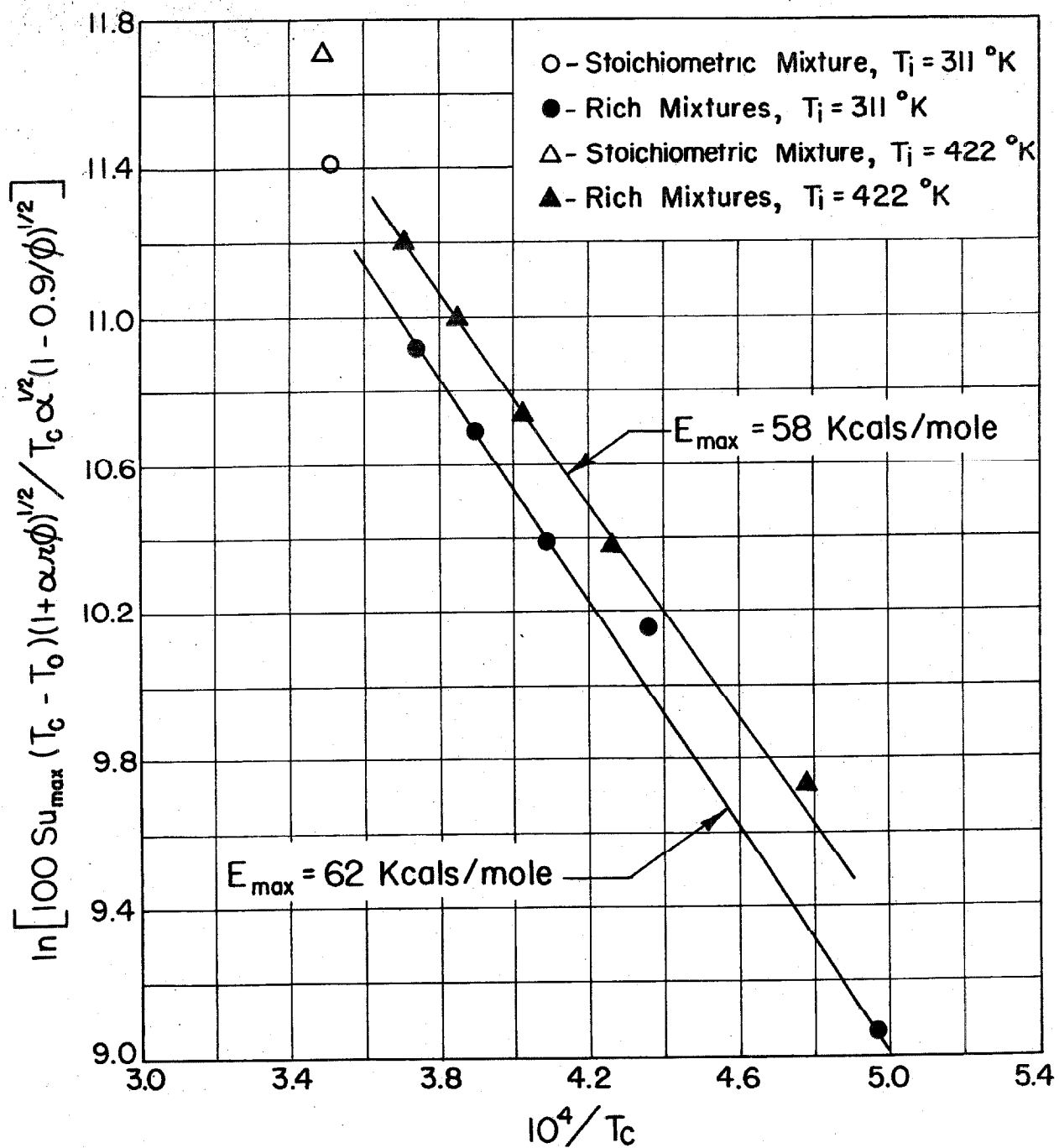


FIGURE 31. PLOT OF $\ln[100 Su_{\max}(T_c - T_0)(1 + \alpha \pi \phi)^{1/2} / T_c \alpha^{1/2}(1 - 0.9/\phi)^{1/2}]$ vs $10^4/T_c$ FOR PROPANE- O_2 - N_2 FLAMES.
($p = 1 \text{ ATMOS.}$, DATA FROM REF. 9)

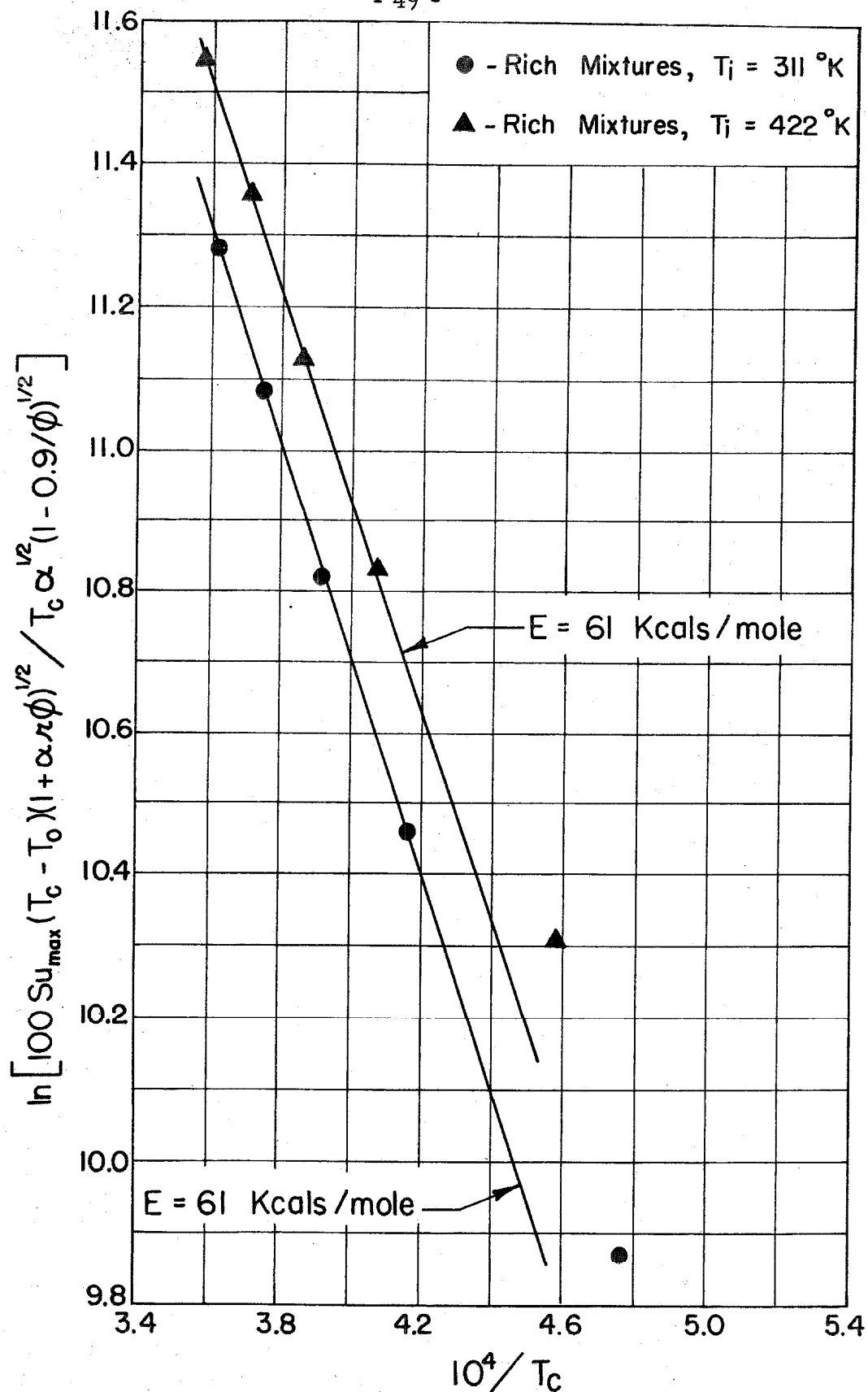


FIGURE 32. PLOT OF $\ln \left[\frac{100 S_{u_{\max}} (T_c - T_0) (1 + \alpha \lambda \phi)^{1/2}}{T_c \alpha^{1/2} (1 - 0.9/\phi)^{1/2}} \right]$ vs $10^4 / T_c$ FOR ETHYLENE - O_2 - N_2 FLAMES. ($p = 1 \text{ ATMOS.}$, DATA FROM REF. 9)